The Mesoscopic Peristaltic Compressor

M. A. Sulfridge and N. R. Miller

ACRC CR-25 January 2001

For additional information:

Air Conditioning and Refrigeration Center
University of Illinois
Mechanical & Industrial Engineering Dept.
1206 West Green Street
Urbana, IL 61801

(217) 333-3115

The Air Conditioning and Refrigeration Center was founded in 1988 with a grant from the estate of Richard W. Kritzer, the founder of Peerless of America Inc. A State of Illinois Technology Challenge Grant helped build the laboratory facilities. The ACRC receives continuing support from the Richard W. Kritzer Endowment and the National Science Foundation. The following organizations have also become sponsors of the Center.

Amana Refrigeration, Inc.
Arçelik A. S.
Brazeway, Inc.
Carrier Corporation
Copeland Corporation
DaimlerChrysler Corporation
Delphi Harrison Thermal Systems
Frigidaire Company
General Electric Company
General Motors Corporation
Hill PHOENIX
Honeywell, Inc.
Hussmann Corporation
Hydro Aluminum Adrian, Inc.
Indiana Tube Corporation
Invensys Climate Controls
Kelon Electrical Holdings Co., Ltd.
Lennox International, Inc.
LG Electronics, Inc.
Modine Manufacturing Co.
Parker Hannifin Corporation
Peerless of America, Inc.
Samsung Electronics Co., Ltd.
The Trane Company
Thermo King Corporation
Valeo, Inc.
Visteon Automotive Systems
Wolverine Tube, Inc.
York International, Inc.

For additional information:

Air Conditioning & Refrigeration Center
Mechanical & Industrial Engineering Dept.
University of Illinois
1206 West Green Street
Urbana, IL 61801

217 333 3115

ABSTRACT

A new design for a meso-scale (miniature) compressor has been developed and analyzed. The term meso is used to describe a device which is smaller than a traditional (i.e. macro) device, and yet larger than the micro devices which have been developed in recent years. This scale of compressor is essential for the development of air conditioning systems small enough to be easily portable and efficient enough to require relatively low power to operate, while still being large enough to do appreciable work. The design under investigation is based on peristaltic action, in which controlled waves are used in rapid succession to propel a fluid down a continuously tapering channel. Electrostatic actuation is used to control the wave. A detailed analysis of this design is performed from an energy standpoint, and many of the major differences between this type of compressor and comparable traditional compressors are highlighted. In addition to the detailed energy analysis, some simple dynamic modeling has also been performed to address transient effects such as squeeze-film damping.

TABLE OF CONTENTS

LIST OF TABLES

Page

LIST OF FIGURES

Page

NOMENCLATURE

Symbol	Meaning
a	channel amplitude
A	area or arbitrary coefficient
B	arbitrary coefficient
C	capacitance or arbitrary coefficient
d	capacitor gap
E	elastic modulus
F	force
h	separation distance or enthalpy
k	relative dielectric constant
ℓ	stretched diaphragm length
$\dot{m}$	mass flow rate
M	mass
n	number of diaphragm pockets
P	pressure
ΔP	total pressure drop from channel entrance to exit
ΔP_n	pressure drop between pockets
q	distributed force or total charge
r	polar displcelment coordinate
R	inlet to outlet volume ratio or total horizontal balloning distance or cavity radius of curvature
S	strained diaphragm line tension
t	diaphragm thickness, or time
u	dimensionless strain equation variable
V	voltage or volume
W	work or width
x	Cartesian coordinate
Δx	horizontal displacement length of diaphragm not in contact with wall
X_{max}	half of channel width

y	Cartesian coordinate
Y_{max}	channel length
z	Cartesian coordinate
z_0	distance from cavity center of curvature to cavity centerline
α	dimensionless parameter used to simplify diaphragm strain equation
β	dimensionless parameter used to simplify diaphragm strain equation
γ	dimensionless parameter used to express diaphragm strain, or the polytropic exponent
ε_0	permittivity of free space
$\varepsilon_{x,y}$	strain in corresponding Cartesian direction
η	dimensionless parameter used to express diaphragm strain
λ	dimensionless diaphragm parameter equal to $\Delta x/\Lambda$
Λ	wavelength of diaphragm
μ	taper slope of channel
ν	Poisson's ratio
ρ	density
$\sigma_{x,y}$	stress in corresponding Cartesian direction

1. INTRODUCTION

1.1 Motivation

Current vapor compression cooling cycles are implemented using a wide variety of system components including a number of different compressors and expansion devices. All such systems share the unfortunate characteristic of lacking portability. There is currently demand for a cooling system lightweight and portable enough to be incorporated as a personal cooling system for an individual. A proposal for a system to meet this demand is outlined rather thoroughly in [1]. The reciprocating diaphragm compressor design proposed for the mesoscopic refrigeration unit described in that proposal is revolutionary. It has no known precedent among successful full-scale refrigeration compressors. The important compressor designs (in terms of commercial success) include:

1. Piston compressors.
2. Rotary compressors.
3. Scroll compressors.
4. Screw compressors.
5. Centrifugal compressors.

With the exception of the centrifugal compressor, which is only used for very large capacity systems, all these compressors employ rigid metal surfaces to compress the refrigerant gas. That is, they are positive displacement compressors. (For a good review of current compressor designs and their application in the refrigeration industry see [2].) Diaphragms are commonly used to pump liquids, but are seldom if ever used to compress a gas. Furthermore, the scroll, screw, and centrifugal compressors all continuously compress the refrigerant from the input to the output of the unit. Only the piston and rotary compressors use the discontinuous compression process as proposed for the reciprocating diaphragm compressor.

1.2 An Alternate Design

This document describes an alternate mesoscopic compressor design. The design still uses a diaphragm as the compression device, but the volumetric compression process is

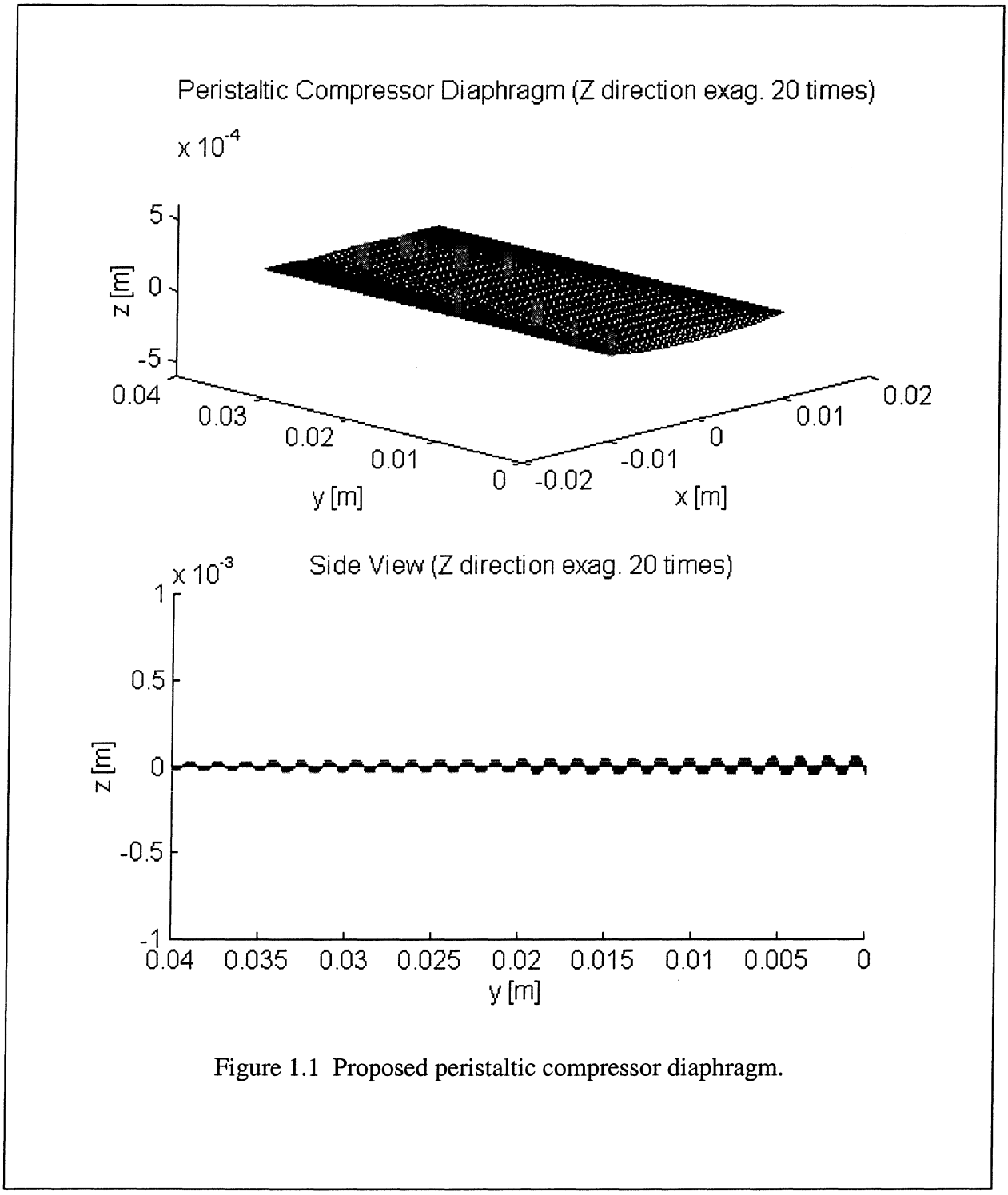

Figure 1.1 Proposed peristaltic compressor diaphragm.

continuous and the amount of volumetric compression per unit length of refrigerant flow can be reduced as much as desired. The design is conceptually very similar to the scroll compressor. That compressor design, while it has existed since the turn of the century, has become practical only during the last decade with the advent of modern

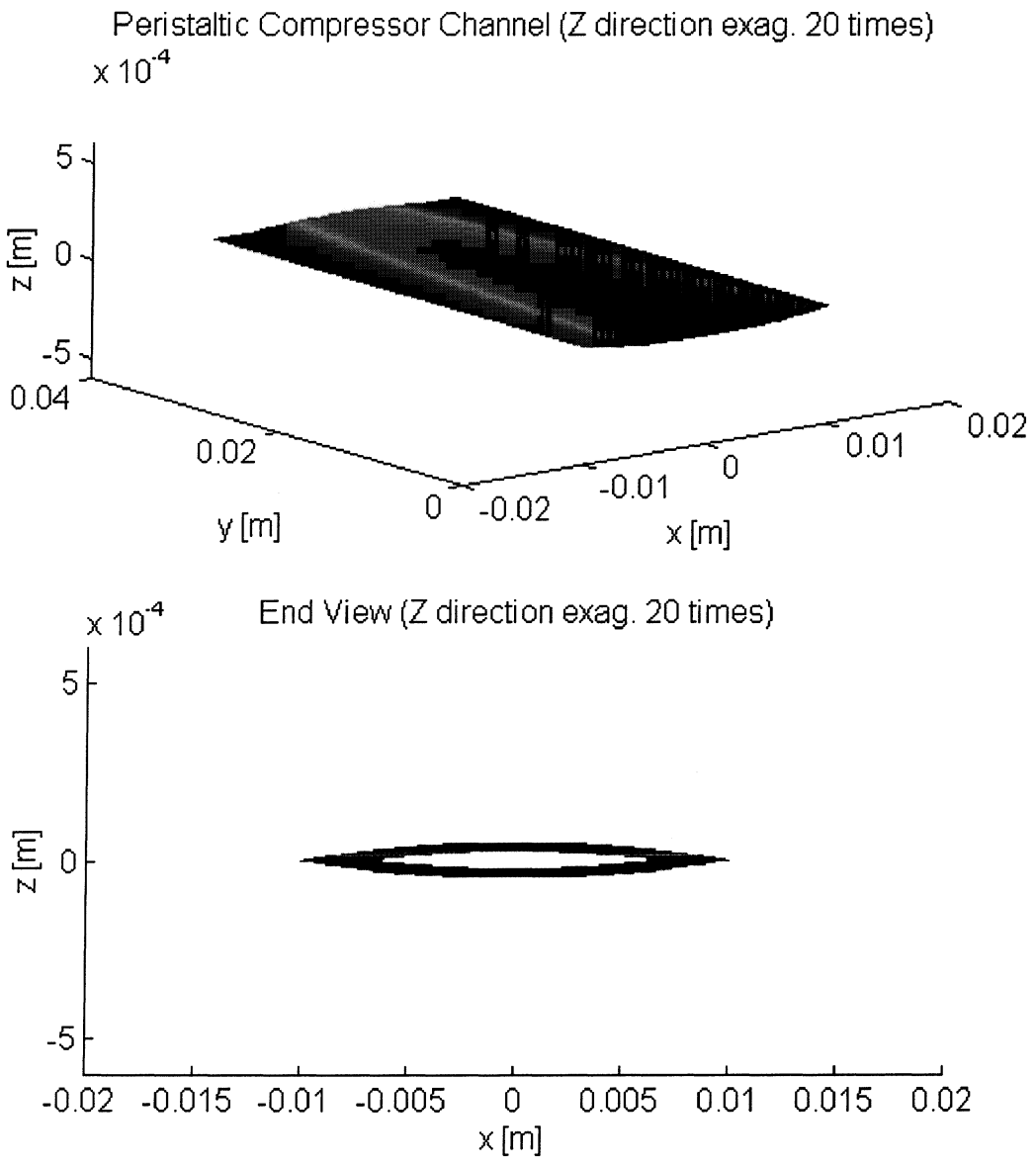

Figure 1.2 Cavity or passage shape for the proposed peristaltic compressor.

manufacturing methods. The scroll compressor is growing rapidly in popularity due to its reliability and efficiency. We have christened our alternative compressor the **peristaltic** compressor**.** This biological term is exactly suggestive of the mode of operation of this compressor. A diaphragm (Figure 1.1) is centered in a passage (Figure 1.2). The passage cross section is something like the proposed cross section of the reciprocating diaphragm compressor. (The shape in this figure is that of a section of a circle with its center linearly moved away from the etched surface. This shape was chosen since it is relatively easy to obtain, and it approximates the natural parabolic shape that a membrane under uniform load would seek.) While the reciprocating diaphragm compressor is circular, the peristaltic compressor is linear. The cross sectional area tapers nearly uniformly from the entrance to the exit. The peristaltic compressor uses the same electric field driving mechanism as the proposed reciprocating diaphragm compressor. The diaphragm is metalized on both sides and operates at ground potential. A series of electrodes are fabricated on the top and bottom surfaces of the passage. The shape of the passage causes "zipping" of the diaphragm just as in the reciprocating diaphragm compressor design. A proper pattern of positive and ground potentials on the passage electrodes deflect the diaphragm into its wave shape. Then, by activating and deactivating the electrodes in the passage, the waves can be made to advance from the large end of the passage toward the small end. (See Figure 2.1)

As can be seen, the advancing waves (the peristaltic action) force the compression of the gas as the channel narrows. The compression is gradual. There is never a large pressure differential between any two "pockets" in the passage. (Indeed, by lengthening the passage, the pressure change can be made as small as desired.) In addition, there is never a large temperature difference between any two pockets. This is an important thermodynamic advantage for this design. It would also be very simple to add heat exchangers along the length of the passage to improve system C.O.P. The design does not require valves. The design has a theoretical clearance volume equal to zero. Finally, both the volumetric flow rate of refrigerant and the volumetric compression ratio are easily controlled through electronic means.

2. DESIGN CONSIDERATIONS

2.1 "Pocket" Shape

A schematic diagram (Figure 2.1) illustrates in a conceptual way how the diaphragm will drive the refrigerant down the compressor passage (cavity). The drawing shows the

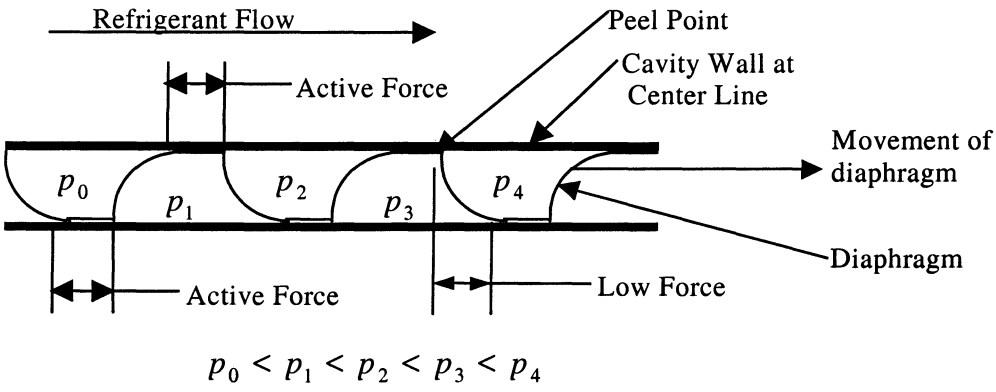

Figure 2.1 Schematic diagram of the cavity cut along the centerline showing the probable shape taken by the diaphragm.

profile of the diaphragm along the centerline of the passage. The refrigerant flows from left to right. As indicated in the figure, the pressure in each succeeding pocket is higher. This will cause the diaphragm to balloon as indicated. The profile pattern is as shown. The compression results from the taper of the cavity walls towards each other from left to right and from top to bottom. This cannot be seen in the drawing. The diaphragm is metalized on both faces and will be maintained at ground potential. Segmented electrodes on the cavity wall will be activated or grounded to enable or disable force generation.

2.2 Control

As mentioned above, a design using a constant wavelength throughout the passage is very simple to control. The same pattern of electrode potentials can be repeated down the length of the passage. Thus the same control signal can be repeated down the passage from one wave to the next. The clocking rate of the pattern cycle sets the volumetric

flow rate. The volumetric compression ratio can also be easily varied by starting the wave pattern in the diaphragm at greater or lesser distances into the passage. Thus to reduce the volumetric compression ratio, the wave pattern would simply be activated deeper in the channel. Nearly infinitely variable control of both the volumetric flow rate and volumetric compression ratio can be realized. In particular, it will be very desirable to build the prototype compressors with excess volumetric compression (that is with overly long channels). That will allow for some margin of error, and yet allow the volumetric flow rate to be adjusted to whatever is required for proper system operation. Control can be based on simple clocked logic generated by discrete logic, a programmable logic device (PLD), or a microcontroller.

2.3 Passage Entrance and Exit

The leading and trailing edges of the diaphragm will have to be supported to prevent damage to the membrane. That is, refrigerant must not flow by an unsupported

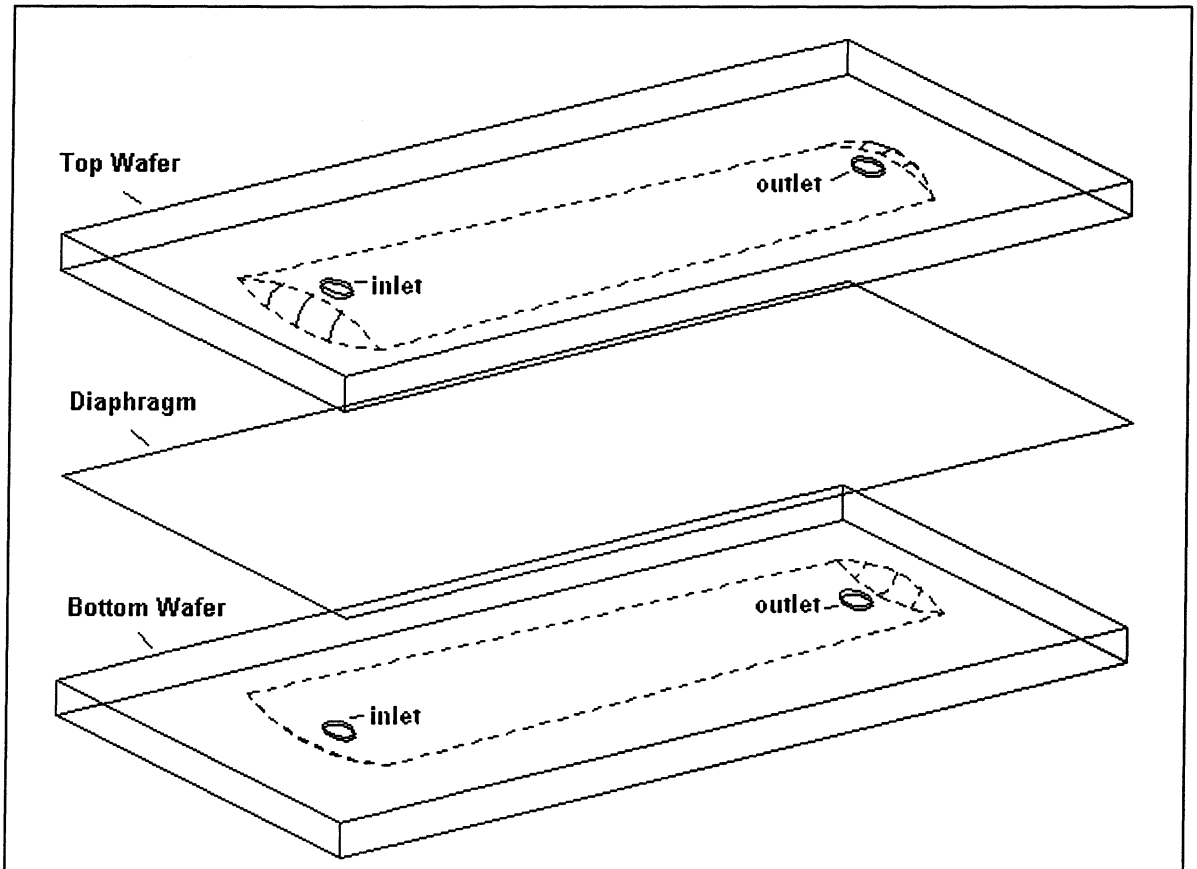

Figure 2.2 Illustration of a method of supporting leading and trailing diaphragm edges.

diaphragm edge on entry or exit. The exact method in which this can be accomplished will depend heavily on the limitations of fabrication technology. A possible method is illustrated in Figure 2.2. From the standpoint of operation of the peristaltic compressor, details upstream and downstream from the inlet and outlet should be of little concern.

2.4 System Issue

When off, the compressor is an open connection between the high and low pressure sides of the refrigeration system. This will permit rapid charge redistribution. In most conventional refrigeration systems, the compressor acts as a fairly effective valve blocking charge migration for a fairly long period of time. This may be an issue if the system is operating at such low loads that it must be repeatedly cycled on and off. Typically, major inefficiencies occur during startup if the charge must be redistributed. It would be possible to leave the electrodes energized during the off cycle to impede charge migration. The only loss would be leakage current across the capacitor plates. The most energy efficient strategy (paying the energy cost of repeated system startups with charge redistribution, or paying the energy cost due to leakage current to maintain the peristaltic compressor in a sealed configuration) will probably have to be determined by experiment. Further, it may be possible to reduce system capacity to such a low level by means of reducing the compressor frequency and/or volumetric compression, that cyclic operation is not needed at all.

2.5 Startup

When shut down with none of the electrodes active, the diaphragm will assume a flat configuration in the center of the passage. Equal pressure will exist throughout the passage. This is unlike current full size compressors. Activating the electrodes to establish a wave pattern should cause minimal pressure change in each pocket but will involve some work due to lateral flow of refrigerant gas (into newly established "pockets"). It is not expected that the minor amount of work done on the refrigerant during startup will impede the formation of the ripple pattern in the diaphragm.

3. ENERGY MANAGEMENT

3.1 Energy Balance

The proper management of energy is of supreme importance to the design of this compressor. The energy available through the type of electrostatic interaction being used by the compressor is quite small. Thus, the design is largely dictated by energy requirements. Clearly, the only energy input into the compressor is electrostatic. In addition, only half of the energy required to charge up the electrodes is available to do work. The other half becomes capacitive potential energy stored by the closed electrodes.

There are four main sources of energy consumption. These are diaphragm strain, compressive work, work required to move the diaphragm subject to a pressure difference, and internal viscous friction losses. It is important to note that of these energy sinks, diaphragm strain is different from the other three. It is only required to be input once, not on a continuous basis as are the other three. The reason for this is that once the diaphragm is in its strained configuration, the total amount of strain in the diaphragm no longer changes. Thus, the strain may be maintained by the capacitive potential energy stored in the closed electrodes. The compressive work term is straight forward, as is the internal friction. This friction term is believed to be quite small, but it will be examined, nonetheless.

The remaining energy consumption term is that required to move the diaphragm through a difference in pressure. This term is subtle, in that it is difficult to see how it is different from the compressive work term. This can be seen, however, by imagining two infinitely large pressure vessels of slightly different pressures separated by a membrane. in order to move the membrane to the higher pressure side, clearly work must be done. However, it is also clear that no compression is done. Thus, the work required is indeed separate from compressive work.

The following sections will discuss all of the energy terms mentioned in this section. In addition, by utilizing the energy information gained, the compressor's final form will be found. The process by which this is done will also be discussed.

3.2 Available Electrical Energy

To find the amount of energy available to do work in our compressor, we will do a simple thought experiment. As shown in Figure 3.1, let us assume our compressor is a parallel plate capacitor whose plates can move relative to each other compressing refrigerant gas between them. Assume that the plates start with spacing h_0 and approach

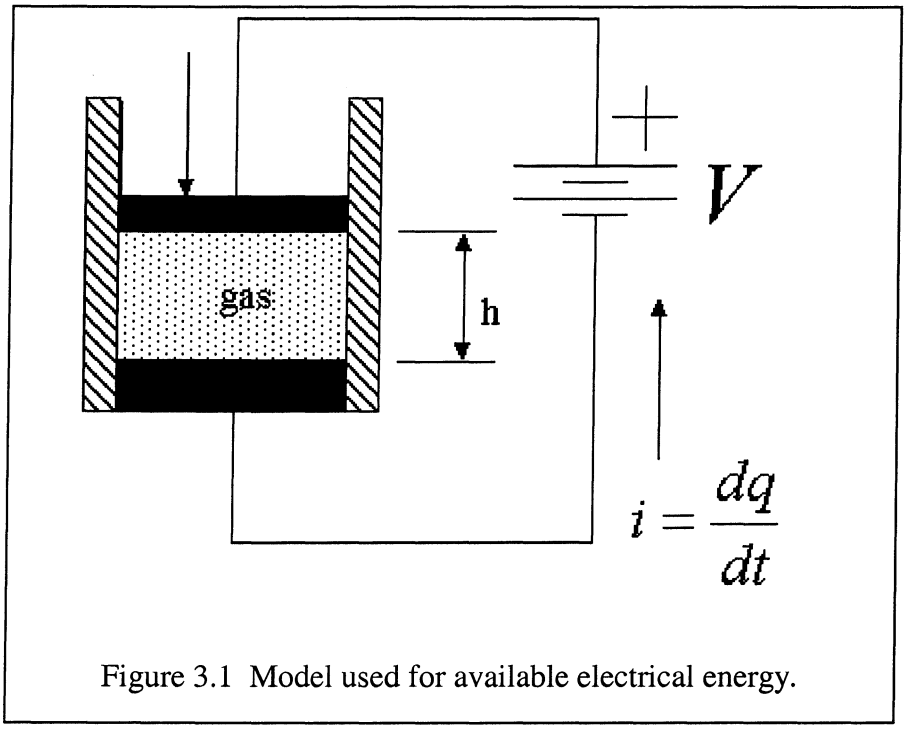

Figure 3.1 Model used for available electrical energy.

to a minimum spacing h_f. Assume that a constant voltage V is applied to the plates. To make things a bit simpler, assume that h_0 is large enough that the initial capacitance, C_0, is negligible. Then, when the constant voltage V is applied, essentially no charge is placed on the plates of the capacitor (that is, $q_0 \approx 0$). Now, as current flows into the plates of the capacitor, the force between the capacitor plates will build compressing the refrigerant gas. Notice that this is a controlled process. Electrical current will be limited by the velocity of approach of the two plates. That is:

$$q = CV$$

$$C = k\varepsilon\frac{A}{h}$$

$$q = k\varepsilon AV\frac{1}{h}$$

$$\frac{dq}{dt} = i = k\varepsilon AV(-1)h^{-2}\frac{dh}{dt}$$

where:

k is the dielectric constant.

ε is the permittivity of free space.

A is the plate area.

$\frac{dq}{dt} = i$ is the current flowing into the capacitor plates.

$\frac{dh}{dt}$ is the velocity of approach of the capacitor plates.

Of course, some energy will be lost through heat as the current flows onto the plates (through wires with non-zero resistance). Further, if the current flow is rapid, some energy will be lost by generation of electromagnetic waves. Let us assume for now that the electric current flow is small so that resistive heating losses and electromagnetic wave propagation are both small. Now, let us see how much electrical work is done as the capacitor plates approach each other. Differential electrical work can be expressed as:

$$dW = Vdq$$

but

$$dq = VdC$$

$$W = V^2\int_{C_0}^{C_f} dC$$

$$W = V^2(C_f - C_0) \approx V^2C_f$$

$$W = V(q_f - q_0) \approx Vq_f$$

Thus, we see that the amount of energy required to charge up the electrodes in CV^2, where C is the capacitance of the capacitor formed by the closed electrode. However, it is well known [3] that the potential energy stored in a capacitor is given by $\frac{1}{2}CV^2$, so that the energy available to do work is also just $\frac{1}{2}CV^2$. Note, however, that as was discussed above, the potential energy can be used to maintain diaphragm strain.

4. GEOMETRY DETERMINATION USING ENERGY

4.1 Channel Cross Section

We have assumed that the cavity wall cross section, for its simplicity of manufacture, is defined to be a section of a circle whose center linearly tapers away from the surface being etched. This is described mathematically by the following function:

$$z = -z_0 + \sqrt{r^2 - x^2}$$

The shape of the upper half of a cavity cross section and the symbols are defined in Figure 4.1 and a projection of the cavity appears in Figure 4.2.

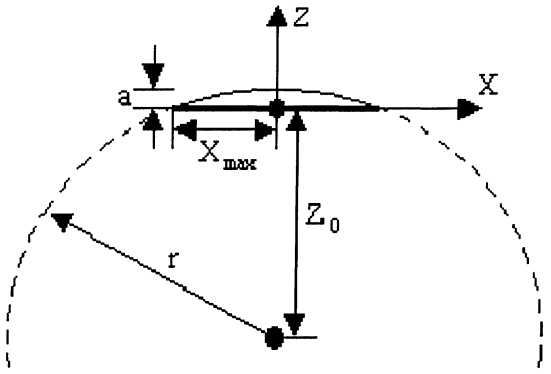

Figure 4.1a Shape of the upper half of the cavity cross section.

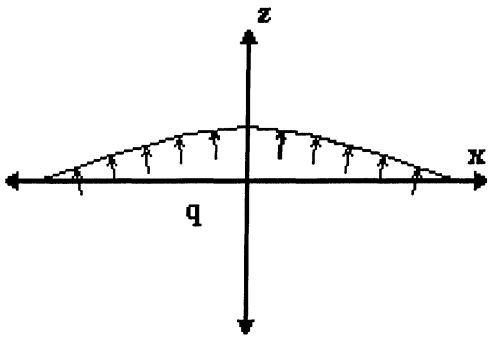

Figure 4.1b Zoom in of relevant portion.

Now let:

Y_{max} be the overall length of the cavity.

n be the number of waves in the cavity.

Λ be the wavelength of the wave.

μ be the slope of the Y axis with respect to the uncut surface.

Then:

$$\Lambda = \frac{Y_{max}}{n}$$

$$z_0 = (r-a) + \mu y$$

$$z = -z_0 + \sqrt{r^2 - x^2} = -z_0 + r\sqrt{1-\left(\tfrac{x}{r}\right)^2} \approx -z_0 + r\left(1 - \tfrac{1}{2}\left(\tfrac{x}{r}\right)^2\right) = (r - z_0) - \tfrac{1}{2r}x^2$$

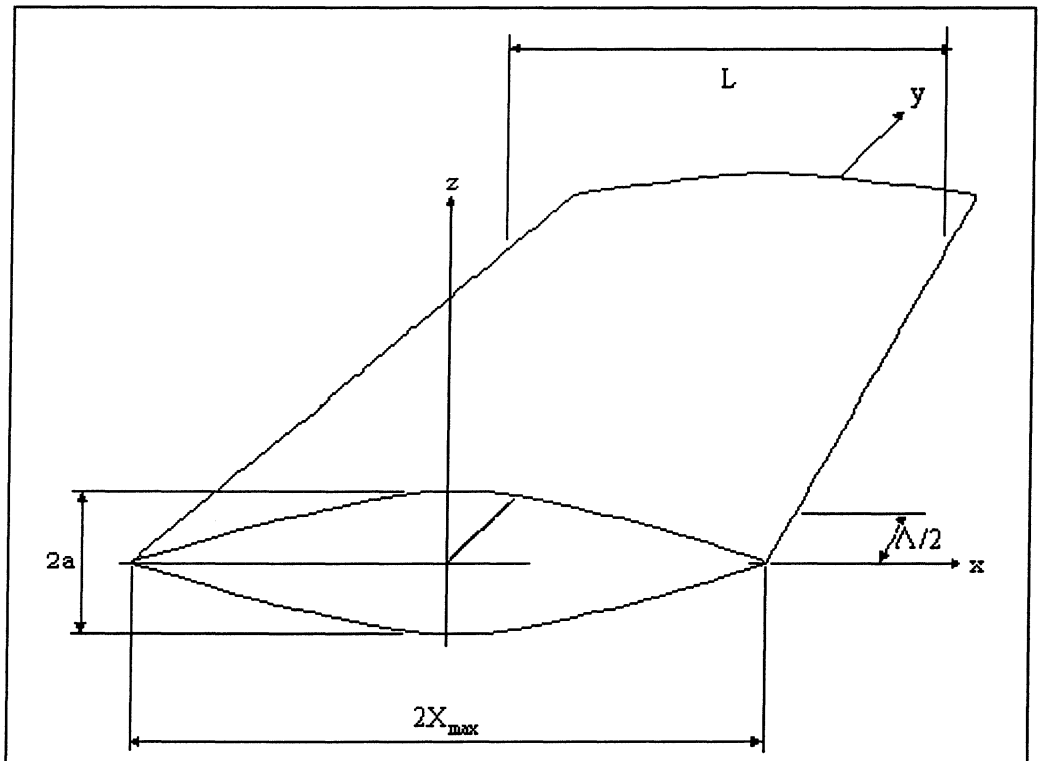

Figure 4.2 Projection of the cavity.

In order to find the actual shape of the channel cross section we will examine a free body diagram of a differential section of the membrane (Figure 4.3). A small angle approximation will be made which is a very good assumption for the geometry that is

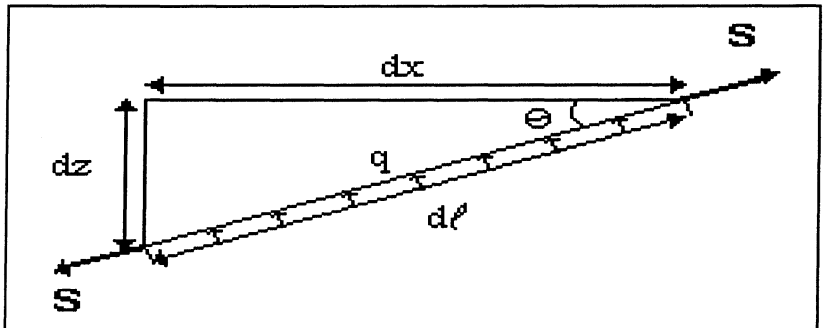

Figure 4.3 Differential piece of Figure 4.1b.

under consideration. We will initially assume a line tension per unit length of the diaphragm, S, that we will later determine.

Doing a force balance in the z direction we have:

$$LS[\sin(\theta)]_1 = LS[\sin(\theta)]_2 + Lqd\ell\cos(\theta)$$
$$\Rightarrow S\left(\sin(\theta)\right]_1 - \sin(\theta)\right]_2\Big) = qd\ell\cos(\theta)$$
$$note\ \sin(\theta) = \frac{dz}{d\ell} \approx \frac{dz}{dx},\ \cos(\theta) = \frac{dx}{d\ell}$$

Thus we must have:

$$-S\left(\left.\frac{dz}{dx}\right|_2 - \left.\frac{dz}{dx}\right|_1\right) = qd\ell\frac{dx}{d\ell} \Rightarrow \frac{d}{dx}\left(\frac{dz}{dx}\right) = \frac{d^2z}{dx^2} = -\frac{q}{S}$$

So the shape the membrane seeks is given by:

$$z(x) = Ax^2 + Bx + C$$

So, given our symetric geometry, we have:

$$z = -A(x-\tfrac{L}{2})(x+\tfrac{L}{2}) = -Ax^2 + \frac{AL^2}{4},\ \text{with } L = L(y),\ L(0) = 2X_{max} \Rightarrow A = \frac{a}{X_{max}^2}$$

So we must have:

$$A = \tfrac{1}{2r},\ A(\tfrac{L}{2})^2 = r - z_0$$
$$\Rightarrow r = \frac{1}{2A},\ L = 2\sqrt{\frac{r-z_0}{A}} = 2\sqrt{\frac{a-\mu y}{A}} = 2X_{max}\sqrt{1-\frac{\mu y}{a}}$$

4.2 Diaphragm Strain

The peristaltic compressor diaphragm undergoes very complex time dependent two-dimensional strain. However, because of the relative dimensions of the compressor, several simplifications can be made which make the strain analysis more tractable. The first simplification is to assume one-dimensional strain. Because each compressor

'pocket' is very short compared with the channel width, the strain along the length of the channel (the x direction) is far greater than it is along the channel's width (the y direction). Because the thickness of the diaphragm (the z direction) is extremely thin compared with both length and width, 2D strain clearly holds. Finally, we assume that the curvature of the channel width is so small that we can take the top and bottom of the channel to be parallel. This assumption clearly overestimates the total strain, and thus it is conservative. Only the first half wavelength of the compressor need be examined,

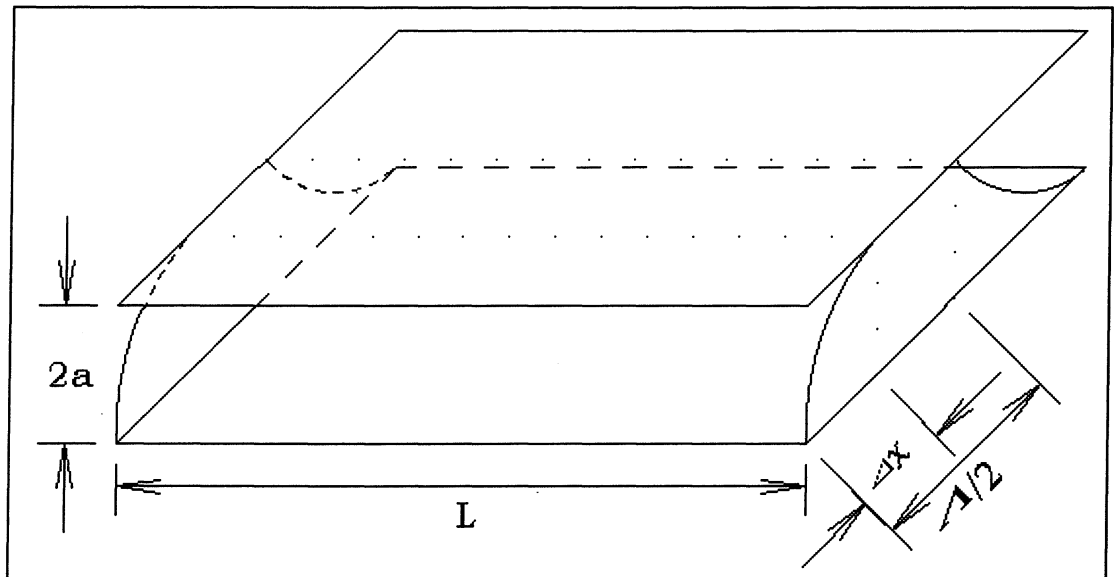

Figure 4.4 Cavity model used for strain calculation.

since each wavelength will have slightly less strain than its predecessor, due to the taper in the cavity. Figure 4.4 shows that portion of the compressor which will be studied.

It is important to remember that the energy required to strain the diaphragm must only be counted once. Even though the strain in the diaphragm is continuously shifting as each wave progresses, the total strain in the diaphragm (along with the total capacitive energy) remains constant after it is initially strained. Thus, the problem of additional capacitive energy needed to do work on the fluid is a separate issue that need not be considered in this section. Therefore there are two different energy balances to be done: the balance of total capacitive energy with strain energy, and the balance of compression energy with added capacitive energy. This section will cover the first of these energy balances.

Note that a side view of the compressor diaphragm looks like Figure 4.5a. In order to simplify things, a transformation of coordinates is used, so that we have Figure 4.5b.

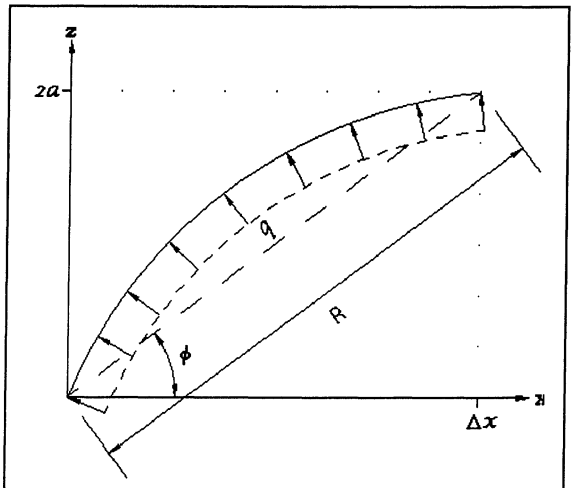

Figure 4.5a Diaphragm 'ballooning'.

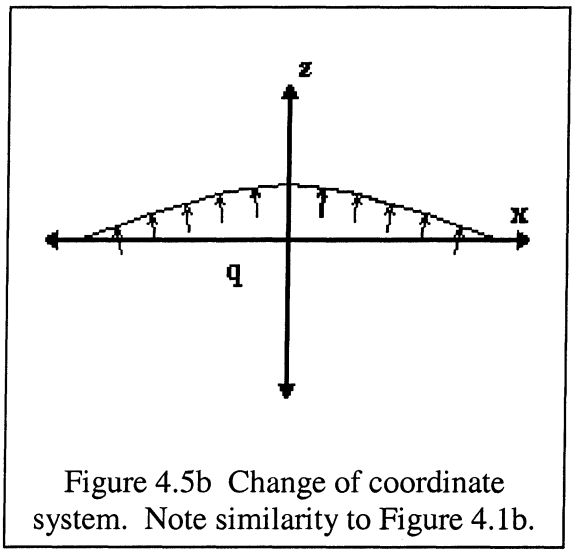

Figure 4.5b Change of coordinate system. Note similarity to Figure 4.1b.

Note that this particular geometry was already calculated to be:

$$z(x) = Ax^2 + Bx + C$$

And we have the boundary conditions:

$$z(0) = 0,\ z(R) = 0,\ R = \sqrt{\Delta x^2 + (2a)^2}$$

So we must have:

$$z(x) = \frac{q}{2S}(R - x)x$$

Now, Figure 4.6 illustrates the unstrained and strained configurations of the

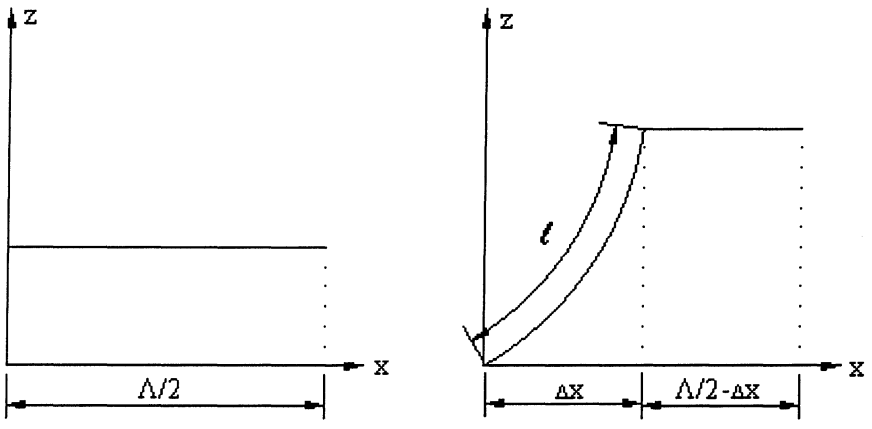

Figure 4.6 Stressed versus unstressed length of diaphragm.

diaphragm for the half wavelength under consideration, so we may calculate the strain in the x direction.

Let:

$$\lambda = \frac{\Delta x}{1/2} \Rightarrow \frac{\Lambda}{2} = \frac{\Delta x}{\lambda}$$

thus:

$$\varepsilon_x = \frac{\left(\ell + \left(\frac{\Lambda}{2} - \Delta x\right)\right) - \frac{\Lambda}{2}}{\frac{\Lambda}{2}} = \frac{\ell - \Delta x}{\frac{\Delta x}{\lambda}} = \frac{\lambda(\ell - \Delta x)}{\Delta x}$$

Now, to find ℓ we simply integrate the arc length:

$$\ell = \int_0^{\ell} d\ell, \text{ where } d\ell = \sqrt{dx^2 + dz^2} = dx\sqrt{1 + \left(\frac{dz}{dx}\right)^2}$$

$$\ell = \int_0^{R} \sqrt{1 + \left(\frac{dz}{dx}\right)^2}\, dx, \text{ where } \frac{dz}{dx} = \frac{q}{2S}(R - 2x)$$

Of course, by our small angle approximation, $\frac{dz}{dx}$ must also be small, so we have:

$$\ell \approx \int_0^{R} 1 + \frac{1}{2}\left(\frac{dz}{dx}\right)^2 dx = \frac{q^2}{8S^2}\int_0^{R} 4x^2 - 4Rx + \left(R^2 + \frac{8S^2}{q^2}\right)dx = R + \frac{R^3 q^2}{24S^2}$$

Substituting this back into our equation for strain we get:

$$\frac{\varepsilon_x}{\lambda} = \frac{R - \Delta x + \frac{q^2 R^3}{24S^2}}{\Delta x} = \frac{1}{\Delta x}\left(\sqrt{\Delta x^2 + (2a)^2} - \Delta x + \frac{q^2\left(\Delta x^2 + (2a)^2\right)^{\frac{3}{2}}}{24S^2}\right)$$

$$= \sqrt{1 + \left(\frac{2a}{\Delta x}\right)^2} - 1 + \frac{q^2 \Delta x^2}{24S^2}\left(1 + \left(\frac{2a}{\Delta x}\right)^2\right)^{\frac{3}{2}}$$

For the geometry we are concerned with, $\frac{2a}{\Delta x} < 1 \Rightarrow \left(\frac{2a}{\Delta x}\right)^2 << 1$, which gives us:

$$\frac{\varepsilon_x}{\lambda} \approx 1 + \frac{1}{2}\left(\frac{2a}{\Delta x}\right)^2 - 1 + \frac{q^2 \Delta x^2}{24S^2}\left(1 + \frac{3}{2}\left(\frac{2a}{\Delta x}\right)^2\right), \text{ let } \alpha = \frac{1}{2}\left(\frac{2a}{\Delta x}\right)^2$$

Thus we have:

$$\frac{\varepsilon_x}{\lambda} = \alpha + \frac{1 + 3\alpha}{24}\left(\frac{q\Delta x}{S}\right)^2, \text{let } \beta = \frac{1 + 3\alpha}{24}$$

$$\varepsilon_x = \lambda\alpha + \lambda\beta\left(\frac{q\Delta x}{S}\right)^2$$

Now, using 2D stress-strain relations, we have:

$$\varepsilon_y = \tfrac{1}{E}\left(\sigma_y - \nu\sigma_x\right) = 0 \Rightarrow \sigma_y = \nu\sigma_x$$
$$\varepsilon_x = \tfrac{1}{E}\left(\sigma_x - \nu\sigma_y\right) = \tfrac{1-\nu^2}{E}\sigma_x \Rightarrow \sigma_x = \tfrac{E}{1-\nu^2}\varepsilon_x$$

And by definition, $S = \sigma_x t$, where t is the diaphragm thickness, so we have:

$$S = \frac{Et\lambda}{1-\nu^2}\left(\alpha + \beta\left(\frac{q\Delta x}{S}\right)^2\right), \text{let } u = \frac{S}{q\Delta x}, \text{and } \eta = \frac{\mathrm{Et}\lambda}{6(1-\nu^2)q\Delta x}$$

So we must have $S = q\Delta x u$, where u is the real solution to $u^3 - 6\eta\alpha u^2 - 6\eta\beta = 0$. This solution is given by:

$$u = \gamma^{\frac{1}{3}} + \frac{4\alpha^2\eta^2}{\gamma^{\frac{1}{3}}} + 2\alpha\eta, \text{ where } \gamma = \eta\left(3\beta + 8\alpha^3\eta^2 + \sqrt{(3\beta)^2 + 2(3\beta)\left(8\alpha^3\eta^2\right)}\right)$$

And going back to our strain equation, we see that it now takes the simple form, $\varepsilon_x = \lambda\left(\alpha + \frac{\beta}{u^2}\right)$. Note that this is actually the final strain in the diaphragm. The initial strain is 0, and for any given time in between, we have $\varepsilon_x = \frac{l-\Lambda/2}{\Lambda/2}$, where l is the length of the membrane at that time. Now, the work required to strain the membrane to a small change in volume, dv, is given by $dW_s = \frac{1}{2}\varepsilon_x\sigma_x dv = \frac{E\varepsilon_x^2}{2(1-\nu^2)}Ltdl$. Note from above that $dl = \frac{\Lambda}{2}d\varepsilon_x$, so we have:

$$W_s = \frac{ELt\Lambda}{4(1-\nu^2)}\int_0^{\varepsilon_x}\varepsilon_x^2 d\varepsilon_x = \frac{EL\Lambda t\varepsilon_x^3}{12(1-\nu^2)}$$

And the work available from the capacitor is given by:

$$W_c = CV^2 = \frac{\varepsilon_0 kAV^2}{d} = \frac{\varepsilon_0 k\left(\frac{\Lambda}{2} - \Delta x\right)LV^2}{d} = \frac{\varepsilon_0 k\Lambda(1-\lambda)LV^2}{2d}$$

Where k is the dielectric constant, and other terms are described in Figure 4.7.

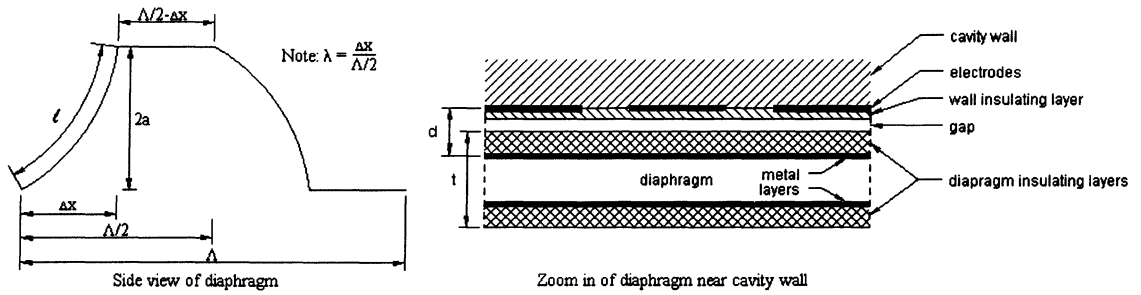

Figure 4.7 Clarification of all important parameters, as well as diaphragm structure.

4.3 Calculation Process

The method by which the compressor channel's size and shape will be calculated is by no means straight forward, and as such it requires some discussion.

The process, in its most basic form is as follows (note that all essential parameters are defined in Figures 4.4 and 4.7). First we note that available capacitive energy is dependent on the parameters d, λ, L, and the voltage, V. Strain energy, on the other hand, depends on a, Λ, and λ. Before any compression takes place, the diaphragm must be strained into its initial configuration. Thus, at this point, Strain energy must be equal to available capacitive energy. The selection strategy is to choose a, Λ, and L. Given this geometry of the compressor cavity as well as the input voltage, this leaves only λ as a variable. Thus, as long as an appropriate startup control scheme is used, λ will be determined by solving the equation $W_s = W_c$.

Note that if we leave some parameter such as V or d unknown, then we have an expression that relates that parameter to λ. This has been done for d using known or calculated values for all other system parameters in order to get an idea of how large this gap can be and still allow the membrane to be strained. Typical results of this can be seen in Figure 4.8. Note that the function of d has a maximum in the allowed interval of

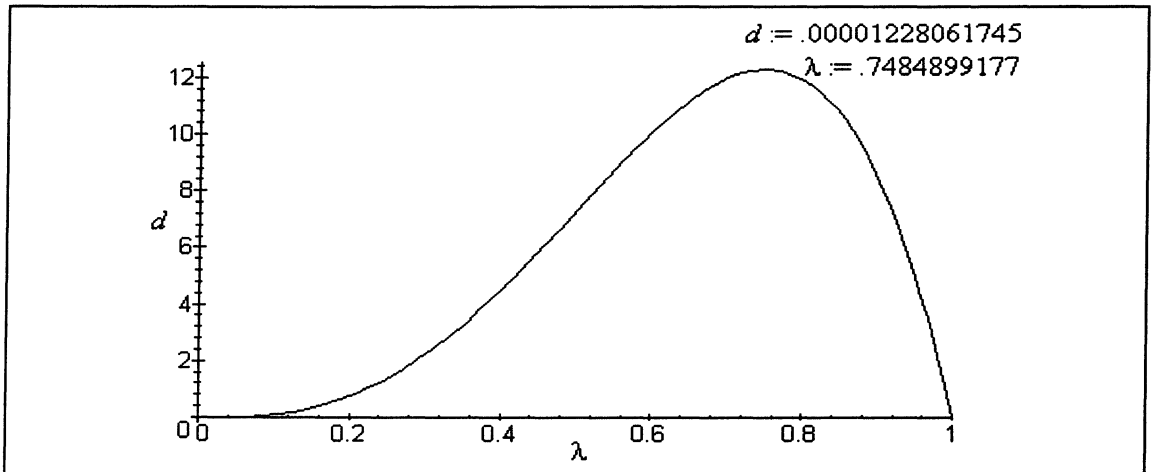

Figure 4.8 Plot of maximum gap values to achieve given value of λ.

$0<\lambda<1$. A compilation of this maximum value of d expressed in microns is shown in Table 4.1 for various channel geometries. Note that in reality this should be a three dimensional table of values for a, Λ, and L, but for the sake of readability, only a two dimensional slice of this table is given. Values used for all other parameters are as follows:

$E = 12.13\,GPa$, $\nu = 0.34$, $k = 2$

$t = 2\,\mu m$, $q = 10\,kPa$, $V = 120\,Volts$

Table 4.1 Maximum possible value of d for various channel geometries.

a(mm) \ Λ(mm)	**0.8**	**1.2**	**1.6**	**2**	**2.4**
0.1	0.00301	0.03429	0.1927	0.7347	2.191
0.0667	0.03429	0.3906	2.193	8.335	24.55
0.05	0.1927	2.194	12.28	45.97	129.0
0.04	0.7349	8.359	46.34	166.1	424.1
0.0333	2.194	24.88	134.7	446.8	1025

Now we can simply check this table to find maximum values of d that are realistic. If none are found, adjust a, Λ, and/or L and repeat the process.

4.4 Channel Length, Taper, and Operating Frequency

How big is the peristaltic compressor and how fast must it operate? There are many design tradeoffs.

Let:

V_1 be the volume of one pocket at the cavity inlet.

V_2 be the volume of one pocket at the cavity outlet.

Note that one wavelength is two pockets long.

So:

$$\frac{1}{2}V_1 = \int_0^{\frac{\Lambda}{2}}\int_{-\frac{L}{2}}^{\frac{L}{2}} z\,dx\,dy = -2A\int_0^{\frac{\Lambda}{2}}\int_0^{\frac{L}{2}}(x^2 - \frac{L^2}{4})\,dx\,dy = \frac{A}{6}\int_0^{\frac{\Lambda}{2}} L^3\,dy$$

let $u = 1 - \frac{\mu y}{a}$, then $L = 2X_{\max}u^{\frac{1}{2}}$

Note that:

$\frac{du}{dy} = -\frac{\mu}{a} \Rightarrow dy = -\frac{a}{\mu}du$

Now when:

$y = 0, u = 1$

$y = \frac{\Lambda}{2}, u = 1 - \frac{\mu\Lambda}{2a}$

So we can further reduce our expression for inlet volume as follows:

$$\frac{1}{2}V_1 = \frac{A}{6}\int_1^{1-\frac{\mu\Lambda}{2a}} 8X_{\max}^3 u^{\frac{3}{2}}\left(-\frac{a}{\mu}du\right) = \frac{4a^2X_{\max}}{3\mu}\int_{1-\frac{\mu\Lambda}{2a}}^{1} u^{\frac{3}{2}}du = \frac{8a^2X_{\max}}{15\mu}\left[u^{\frac{5}{2}}\right]_{1-\frac{\mu\Lambda}{2a}}^{1} = \frac{8a^2X_{\max}}{15\mu}\left[1-\left(1-\frac{\mu\Lambda}{2a}\right)^{\frac{5}{2}}\right]$$

In a similar fashion, the expression for outlet volume is:

$$\frac{1}{2}V_2 = \frac{8a^2X_{\max}}{15\mu}\left[u^{\frac{5}{2}}\right]_{-\frac{\mu Y_{\max}}{a}}^{-\frac{\mu(Y_{\max}-\Lambda/2)}{a}} = \frac{8a^2X_{\max}}{15\mu}\left[\left(1-\frac{\mu(Y_{\max}-\Lambda/2)}{a}\right)^{\frac{5}{2}} - \left(1-\frac{\mu Y_{\max}}{a}\right)^{\frac{5}{2}}\right]$$

Finally, the volume ratio, R, is:

$$R = \frac{V_1}{V_2} = \frac{\frac{1}{2}V_1}{\frac{1}{2}V_2} = \frac{1-\left(1-\frac{\mu\Lambda}{2a}\right)^{\frac{5}{2}}}{\left(1-\frac{\mu(Y_{\max}-\Lambda/2)}{a}\right)^{\frac{5}{2}} - \left(1-\frac{\mu Y_{\max}}{a}\right)^{\frac{5}{2}}}$$

Now, if we specify,

$$X_{\max},\quad \Lambda = \frac{Y_{\max}}{n},\quad Y_{\max},\quad R$$

then we can solve for μ. We know R since we can calculate the input and output volume flow rates from the desired refrigeration capacity and the given temperatures of evaporation and condensation. The ratio of the input the output volume flow rate is numerically equal to R.

The following are some preliminary computations. All calculations are based on the operating criteria listed in the original DARPA proposal. We assume a channel 40 mm long, 20 mm wide, and 0.1 mm thick (a=0.05 mm) at its largest point. Note that it would be possible to break the 40 mm channel into two (or more) sections if that were desirable to reduce the longest dimension of the compressor. We further assume a maximum pressure difference between any two pockets of 0.01 MPa. The pressure difference is a conservative value to be used until a better idea of the maximum permissible pressure differential has been developed. Thus we have:

$X_{\max} = 10mm$

$Y_{\max} = 40mm$

$a = 0.05mm$

$\Delta P_n = 0.02MPa$

$n = \frac{\Delta P}{\Delta P_n}$

Results for three refrigerants are shown in Table 4.2. In all cases, we assume an inlet temperature of $17°C$ and an outlet temperature of $55°C$. The pressure ratio is taken as the saturation pressure at each temperature. A three watt cooling capacity is assumed and used to compute the inlet and outlet volume flow rates.

Table 4.2 Number of cycles and frequency for several refrigerants

Refrigerant	P_{in} MPa	ΔP MPa	Vol. Flow Rate-ml/s	Volume Ratio- R	n - No. of cycles/40mm	Frequency -Hz
R718	0.001935	0.01573	89.98	4.8929	1	2058
R600a	0.2764	0.4886	1.75	2.8313	25	827
R134a	0.521	0.97	0.92	2.9013	49	849

So for a compressor designed for the use of R134a, we would need 49 waves in the 40mm channel and the wave frequency would have to be 849 Hz. Increasing the thickness would reduce the frequency as would changing the compressor width or increasing the pressure difference between pockets.

5. OTHER ENERGY ISSUES

5.1 Viscous Energy Dissipation

One possible cause of energy loss in this compression scheme is that of viscous energy dissipation. The kinetic energy of a viscous fluid can be lost to heat in much the same way that an automobile's kinetic energy is lost to heat due to the friction of its brakes. Many texts (see [4]) examine the effects of fluid viscosity. For very narrow chambers, this energy dissipation is much greater than for traditional large scale systems, and as such it is examined here.

In order to calculate viscous energy losses, several simplifying assumptions will be made to the compressor channel model. First, the channel dimensions are taken to be the average height and width of the channel. Since the taper slopes of the channel dimensions are very small, this assumption is quite reasonable. Second, the channel cross section is taken to be an ellipse due to the fact that hydraulic diameter data are readily available for elliptical channels, and this shape approximates the true cavity cross section very well. Finally, the flow is assumed to move through the channel as though the diaphragm were not present. While this is not a very accurate description of the flow, it does provide a reasonable first approximation, and it makes the problem far more tractable than it would be otherwise. Because of these assumptions, the results obtained should not be taken as an exact value, but should provide an answer that is accurate to within an order of magnitude.

Given these approximations, the pressure drop due to viscous effects is given by the following equation,

$$\Delta P = \frac{\dot{m}}{\rho}\frac{4\mu}{\pi}\left(\frac{a^2+b^2}{a^3b^3}\right)$$

where a and b are the semi-minor and semi-major axes of the ellipse, respectively; $\dot{m}$ is the mass flow rate, ρ is the refrigerant density, and μ is the refrigerant viscosity. Taking the geometric values calculated earlier for the compressor using R134a as the refrigerant, the ΔP calculated is on the order of 1kPa. This amounts to less than 0.2% of the compressor inlet pressure. Thus, even if the actual figure is an order of magnitude higher, these losses do not provide an appreciable contribution to the compressor's energy consumption. Figures for Isobutane are very similar.

5.2 Compressive Work

Now that we have found that the diaphragm can be strained into its initial position, the next step is to see if there is enough power available to continuously compress the fluid. This analysis is done via an energy balance during half a period of compression over the entire compressor. Specifically, the capacitive energy added to each 'pocket' during this period is compared with the sum of two other energies: the energy required to compress that 'pocket' from its initial to its final volume, and the energy required to move the diaphragm through the induced pressure gradient. This analysis is done on the diaphragm after the pressure gradients have already been established through the entire length of the compressor channel, since the work required to build up this gradient is clearly less than doing work on the fluid once the gradient has already been established. It is purely numerical, since the complex geometries involved would make any analytic solution completely intractable.

In order to understand what work is actually being considered here some discussion is probably necessary. First of all, note that once the diaphragm has been initially strained, no further strain energy is required. This is because the elastic membrane stores this energy, and at any given time, the same amount of the diaphragm is being released from its strained state as is being strained, so that no net strain work is done.

The capacitive energy, on the other hand, is a different story entirely. Capacitive energy is continuously being added to the system, but none is ever taken away. This may

seem strange, but once the situation is examined carefully it is obvious. Capacitive energy is added to the fluid (i.e. work is done on the fluid by the capacitor) as charge builds up on the diaphragm and the electrodes as they approach each other. Once the diaphragm makes contact with the wall, this position is held for a short time, and then the electrodes are shorted to the diaphragm potential, so that as the diaphragm moves away from the electrodes, no charge differential is present, and thus no electrical work is done.

The work done on the fluid is straightforward. The simple concepts used here may be found in any number of fluids texts, [5] for example. As each pocket of fluid moves through the channel, it experiences a small change in volume due to the taper of the cavity. If we were dealing with isentropic compression, we would simply have $P_1V_1^{\gamma} = P_2V_2^{\gamma}$, and the work done would be $W = \frac{P_1V_1}{\gamma}\left(1-\left(\frac{V_1}{V_2}\right)^{\gamma-1}\right)$. Since this condition is not quite true, the actual situation is slightly different, but this approximation will at least get us close.

The other work required is that of moving the diaphragm through a pressure gradient. This term is the one that makes having multiple 'pockets' so beneficial. The more 'pockets' there are, the less the pressure gradient, and thus the smaller the force that the diaphragm has to push against. This work, over the course of half a period, is simply $W=L\Lambda a\Delta P\cos(\theta)$ where $\theta=\arctan(2a/\lambda\Lambda)$ is the angle the diaphragm makes with the cavity wall. This may not seem obvious, but a careful study of how each differential piece of the diaphragm moves over the course of half a period reveals it to be true. Clearly, in a full period, each piece of the diaphragm must end up back where it started. Thus it must have moved through two full channel heights, $4a$. Therefore, by symmetry, over half a period it must have moved through one channel height, $2a$.

Now, in order for the compression to work, the capacitive energy available must be greater than the work required by each 'pocket'. Unfortunately, with a previously selected channel geometry of a=50 μm, Λ=1.6 mm, and L=20 mm, this requires at least a

170-Volt system if the final capacitor gap, d, is 0.3 μm. This work comparison is shown in Figure 5.1.

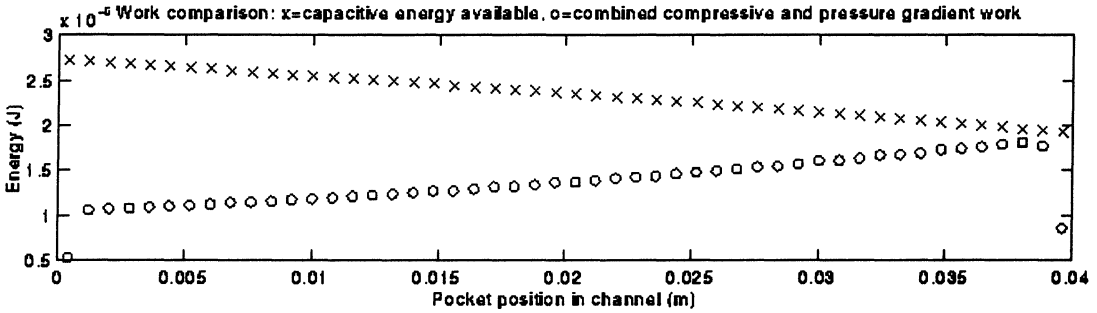

Figure 5.1 Comparison of available and required energy for compression as a function of channel position.

Notice how the work required goes up as a function of channel length, while the available work decreases. This pattern is due to the assumed linear taper of the channel, which was chosen because of its simplicity of manufacture. Clearly, this is not optimal. It would be far better to make these lines parallel, in which case we could reduce the input voltage to make the two energy profiles identical. By doing so, simulation has shown that the input voltage could be lowered to around 140 Volts. It would be troublesome to actually modify the channel geometry to accomplish this due to manufacturing difficulty. However, an effective change in taper rate could be achieved by varying the rate at which electrodes were activated as a function of channel length, or alternatively by varying the width of the electrodes. The latter method would be preferable since it would preserve the simplicity of the control scheme, which is to apply the same input signal to each electrode with a phase shift on each that is an obvious function of channel length. Varying the width of the electrodes is not too difficult, since it is effectively just a change in circuit layout. The issue of exactly how this width should vary will require further study.

5.3 Possible Benefit of Heat Transfer

A typical refrigeration cycle is shown in Figure 5.2. The three lines illustrate three compression processes. The dotted line from A to B represents an idealized, isentropic compression [i.e. reversible (quasistatic) compression with no heat exchanged

(adiabatic)]. A real process, such as the one proposed for the reciprocating diaphragm

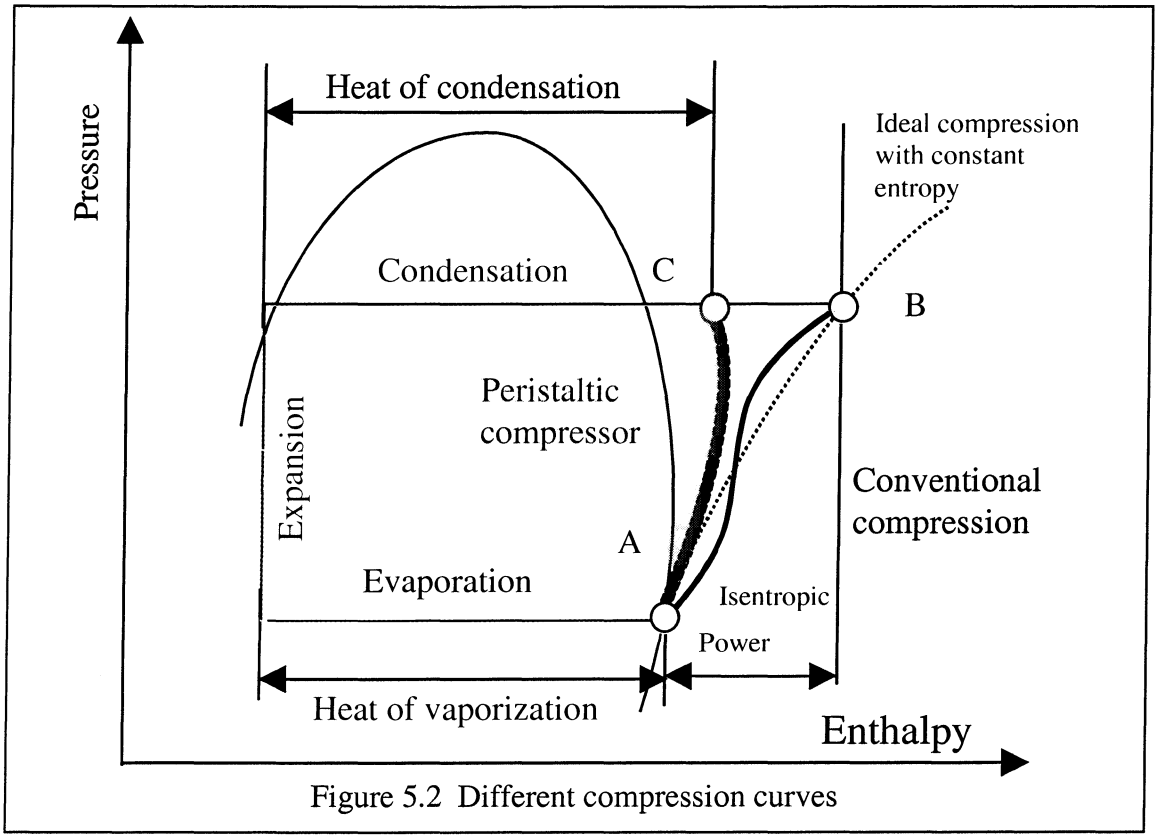

Figure 5.2 Different compression curves

compressor, (illustrated by the solid line linking A and B) is neither quasistatic nor adiabatic. However, the entropy of the discharge gas of the real compressor falls very near to the inlet entropy. The solid line indicates the influence of the heat exchange during the compression. Initially the compressor is insulated to prevent heat transfer into the compressor. At some point the fluid becomes warmer than the cavity walls and the insulation is removed to allow heat flow out of the compressor.

Compression with continuous cooling of the gas is indicated by line A-C. This is the process that could be realized in the proposed peristaltic compressor when in contact with the external environment (heat sink). In simple terms the peristaltic compressor allows the cooling of the refrigerant gas during the compression thus supplying cooler denser refrigerant at the compressor outlet. A schematic diagram is shown in Figure 5.3. Arrows show the direction of heat flux.

Based on the exciting prospects of the possible benefit of heat transfer in the

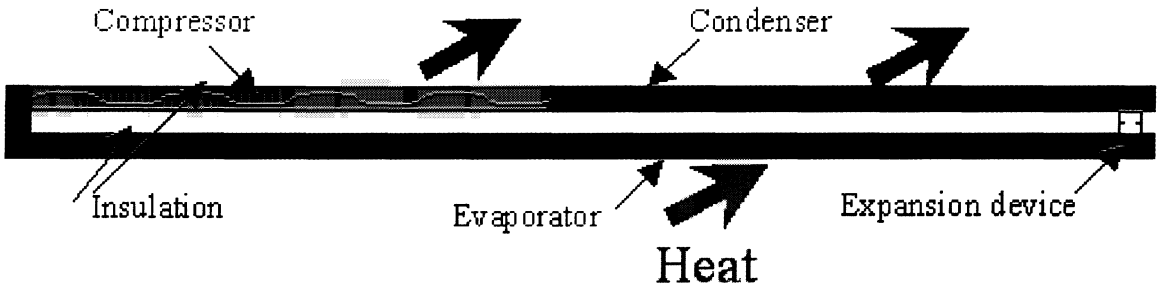

Figure 5.3 A possible system layout showing heat transfer directly to the environment from the peristaltic compressor during the compression process.

compression process, several simulations were run using real refrigerant data for both R134a and R600a, along with calculated channel geometry for the respective refrigerants. The simulations were based on insulating (i.e. adiabatic) the compressor until the refrigerant temperature rose above the ambient temperature, and at that point allowing heat transfer. The calculated flow rates made it clear that it was laminar flow, so laminar equations were used in calculating the heat transfer coefficients for each pocket. In reality, due to the inherent circulation that will occur in each pocket of the compressor because of the way it operates, the heat transfer should be higher than the laminar equations predict. However, as a conservative estimate the laminar equations should be quite reasonable.

The results of a simulation for R134a at 5°C superheat are shown in pressure-enthalpy diagram form in Figure 5.4. Note that there are three 'stages' to the compression. The first stage is typical isentropic compression. This is the stage where the compressor is insulated. The second stage is where beneficial heat transfer starts to occur, and the third stage is when the refrigerant fluid enters the vapor dome, at which point compressor energy goes almost entirely into converting the refrigerant from vapor to liquid. This occurs due to the fact that heat transfer holds the temperature of the refrigerant nearly constant, and inside the vapor dome, temperature and pressure are one-to-one related. It is believed that compression should actually be halted as soon as the refrigerant enters the vapor dome due to the fact that at that point heat can most efficiently be removed by the

condenser. Therefore it would be highly desirable to be able to detect when this transition takes place.

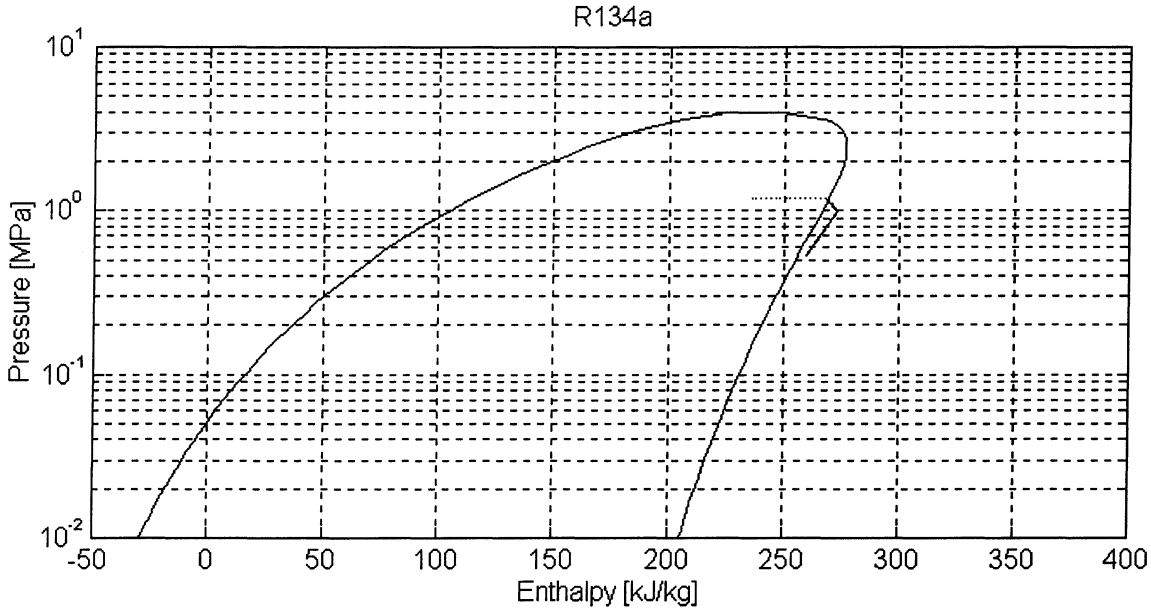

Figure 5.4 Compression path with heat transfer for R134a.

Fortunately, Figure 5.5 illustrates a very simple way to do this. Figure 5.5 is the same type of work distribution diagram shown in Figure 5.1. The main difference is that this

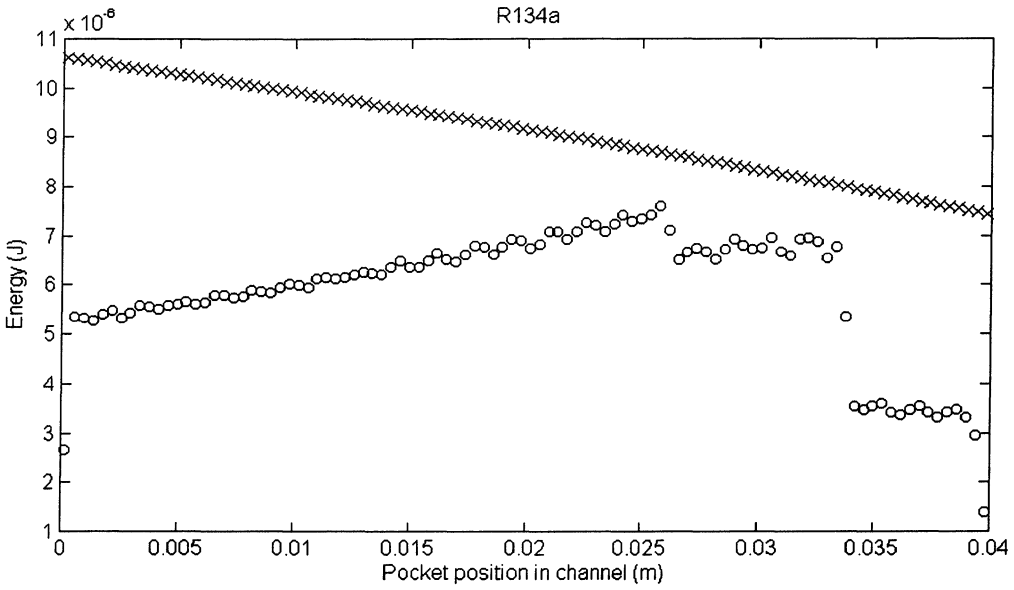

Figure 5.5 Energy comparison for compression with heat transfer on R134a.
x = available energy, o = required energy

data was gained from the simulation in which heat transfer is allowed to take place. Once again the three stages of compression are clearly visible in the diagram. In this case the transitions are clearly marked by jump discontinuities in the energy load required by the compressor. The first jump shows the benefit of heat transfer in compression. It allows for a nearly 50 Volt reduction in the required voltage. The second jump, which is markedly larger, is the point at which the refrigerant enters the vapor dome. By sensing the current at each electrode (i.e. using the electrodes in the dual role of actuators and sensors) it would be quite easy to find the point at which the current dropped by a significant amount. At that point compression could be halted by simply not actuating any of the electrodes past that location in the channel.

The significant energy benefit gained from heat transfer is not the same for all

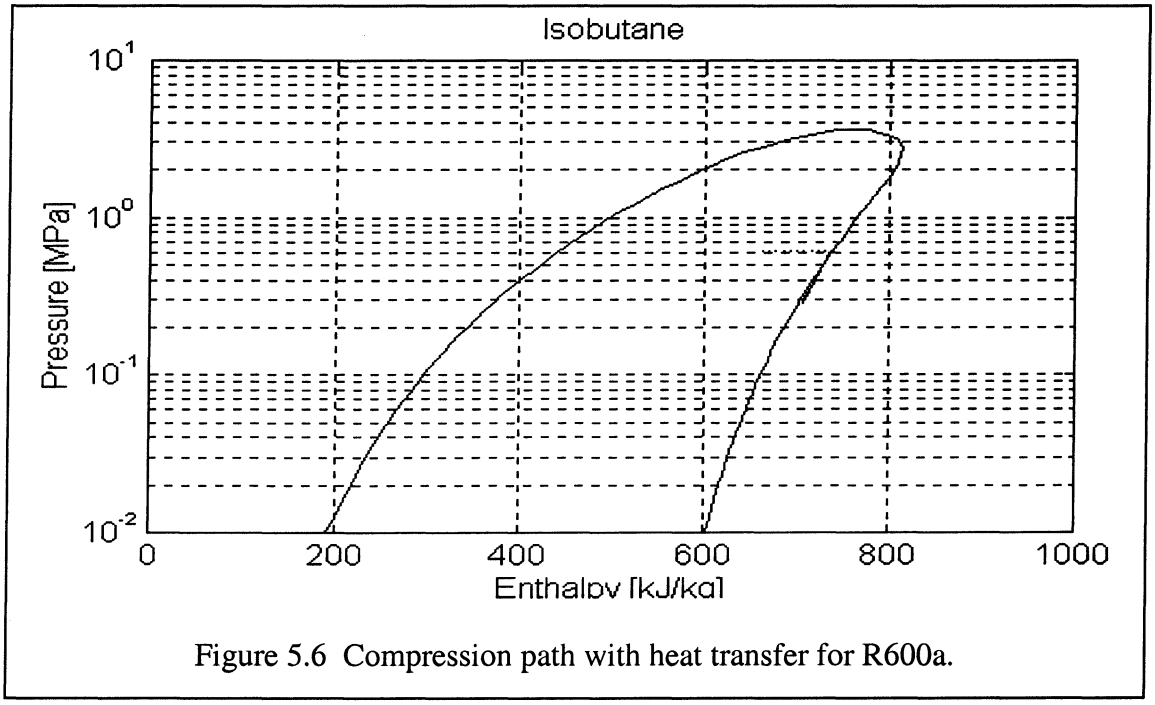

Figure 5.6 Compression path with heat transfer for R600a.

refrigerants. It does allow the simple method of detecting the vapor dome described above for all refrigerants. However, a few refrigerants, including R600a, have the interesting (and quite useful) characteristic that their constant entropy lines converge with the vapor dome as pressure increases, rather than diverging, as is the case with most refrigerants. The result of this interesting feature is that even in isentropic compression, unless the inlet refrigerant is significantly superheated, the compression path never

significantly diverges from the saturated vapor line. Thus, in the case of using heat transfer in the compression process for R600a, entry into the vapor dome and the point at

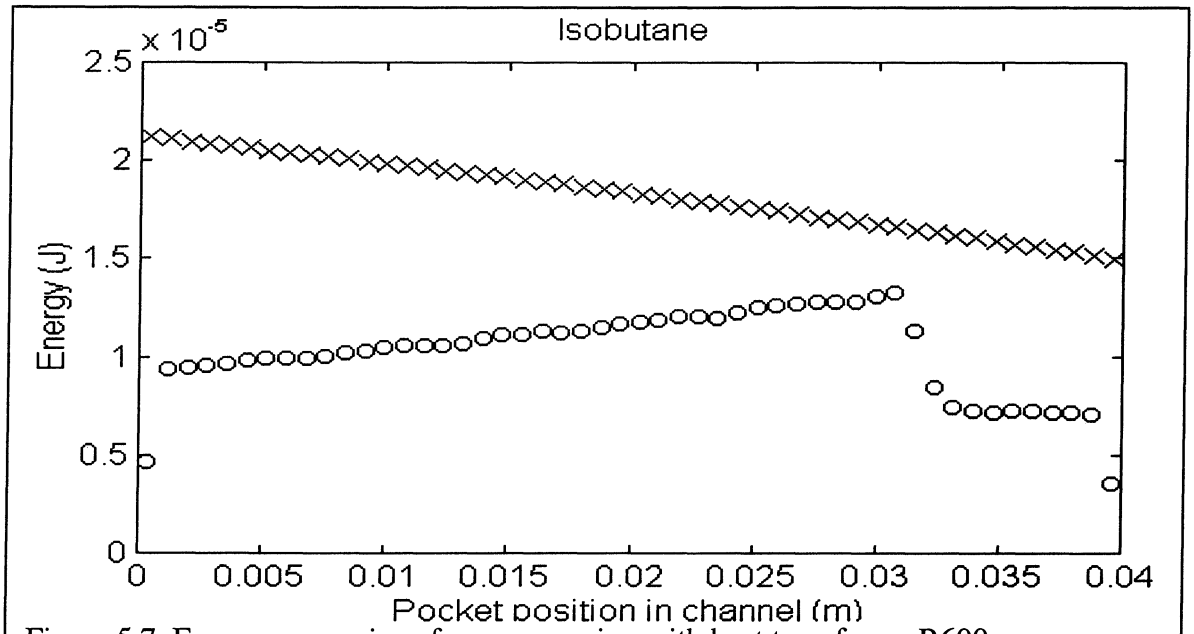

Figure 5.7 Energy comparison for compression with heat transfer on R600a.
x = available energy, o = required energy

which beneficial heat transfer begins are nearly coincidental. Figures 5.6 and 5.7 illustrate this point quite nicely.

Note that for R600a, there are only two 'stages' to the compression. The initial adiabatic stage, followed by the heat transfer stage coupled with the refrigerant entering the vapor dome.

6. ACTUATION AND CONTROL

6.1 Alternative Electrode Actuation Strategies

The basic proposed cavity shape assumes the use of uniformly spaced electrodes on the cavity walls. The electrodes would be actuated in such a way as to produce constant wavelength "ripples" in the diaphragm. Such a design leads to particularly simple electrode control. (The pattern of electrode activation voltages would repeat for every wavelength down the length of the cavity.) Other designs are possible. For example, a cavity of uniform cross section could be used if the wavelength of the diaphragm ripples diminished down the length of the cavity. It might also be desirable to diminish only the width or only the depth of the cavity with length. All of these possibilities must be explored.

6.2 Electrode Resolution

The number of electrodes per wavelength may be an issue. Due to the segmented electrode design, the device is ultimately discrete. Waves advance in discrete steps, the size of those steps is a function of the size of individual electrodes. The step action is bound to cause some losses due to compression cycling (over compression followed by slight decompression). As the number of electrodes per wavelength increases, the losses associated with this effect will approach zero. Even with relatively large electrodes, the effect may not be too important if the actuation and release of electrodes on the trailing and leading edges of the "pocket" respectively can be coordinated properly. This issue will be explored as the analytical and experimental tools are developed.

In addition, in order to assist in the zipping action of the electrodes once compression has begun, the electrodes need not be purely linear. By interleaving the electrodes as shown in Figure 6.1, significant gains in the effectiveness of zipping can be realized, since part of the next electrode will already be in contact with the cavity wall when it is

activated. If it is necessary to place the electrodes in the diaphragm as well as on the

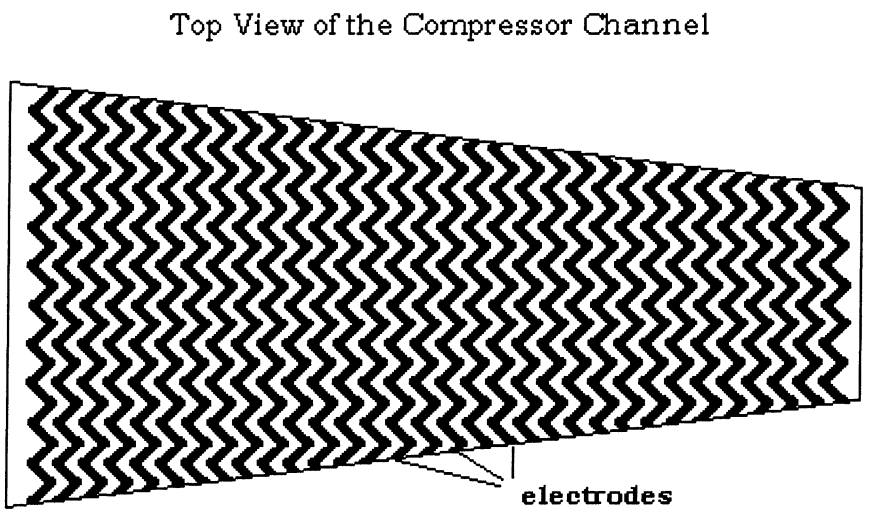

Figure 6.1 Conceptual view of interleaved electrode patterning to assist with zipping.

walls of the channel, this type of pattern would also be effective in minimizing the strain in the electrodes.

7. DIAPHRAGM DYNAMICS

7.1 Potential "Squeeze Film" Problem

Concerns about the effect of the "squeeze film" phenomenon have been raised. As the diaphragm approaches the cavity wall, refrigerant gas will tend to impede its approach. Simply put, the gas cannot get out of the way in time. This is a dynamic phenomenon. As the compressor operating frequency increases, the "squeeze film" can be expected to grow thicker. The gas film between the diaphragm and the cavity wall would increase capacitor plate spacing and change the dielectric constant. Some compression losses will also occur (similar to the conventional clearance volume problem). If compressor operating frequencies can be kept reasonably low, the problem may be minor.

A search of the literature has not uncovered a solution to what is essentially a foil squeeze film bearing (see chapters 6 and 8 of [6]). Further, ultra thin refrigerant gas films will exist in the compressor. Under conditions of extremely thin gas films, molecular effects become important and the classic Reynolds equations no longer apply (see page 58 of [6]). Reference [7] indicates that the load which can be supported by an oscillating slider riding on an ultra thin gas film is over predicted by the classic Reynolds analysis. Thus, it is likely that calculations of the time needed to reach a certain film thickness based on classic Reynolds analysis methods will be conservative. The Knudsen number (Kn) for a one micron refrigerant gas film is about 0.06. Kn below 0.01 indicates that the Reynolds solution applies, while Kn above 15 implies that molecular flow dominates and the Reynolds solution is completely inaccurate. In the case of the peristaltic compressor, we would expect the Reynolds solution to be slightly conservative.

While a solution to the problem of a flexible film being pulled toward a rigid wall has not been uncovered, many solutions to the problem of films squeezed between closely spaced rigid plates appear in the literature. In reference [6], (see page 637), it is explained that inclined surfaces (as occur in the peristaltic compressor as the diaphragm approaches the cavity wall) have lower squeeze film effect than do parallel plates since

the gas can more easily flow from between the approaching surfaces. Unfortunately, the pressure between the diaphragm and the cavity wall will distort the diaphragm and tend to trap refrigerant (see [8]).

One typical solution for rectangular plates is presented in [8]. That solution can be represented as a linear damper with a damping coefficient which is a function of the plate gap. That is, the force between the plates can be represented by the following expression:

$$F = \beta(h)\frac{dh}{dt}$$

where:

F is the force acting to resist the squeeze action of the plates.

h is the gap between the plates.

$\frac{dh}{dt}$ is the gap closing velocity.

$$\beta(h) = -\frac{96}{\pi^4}\mu\frac{L^3W^3}{L^2+W^2}\frac{1}{h^3}$$

L, W are the length and width of the plate.

Table 7.1 Viscosities of various refrigerants at operating conditions.

Refrigerant	**Viscosity** [Pa-s]
R600a	7.47e-06
R134a	1.17e-05
Steam	9.63e-06

μ is the viscosity of the gas.

Viscosities for our three refrigerant gases are given in Table 7.1.

It should be noted that every solution found in the literature shows the damping coefficient inversely proportional to the cube of the plate gap. This means that if the diaphragm approaches the cavity wall at constant velocity, the force acting to impede the approach rises very rapidly as the gap drops below a few microns.

7.2 A Simple Model of System Dynamics

All of the compression analysis is predicated on the ability to get the capacitor gap size, d, in the neighborhood of 0.5 μm. This is technically feasible only if the actual gap between insulating layers on the diaphragm and cavity wall (see Figure 12) goes to zero in the amount of time it takes for the wave to advance one electrode width forward. Otherwise, equilibrium flow will be reached with a gap between these insulating layers, which by themselves are already on the order of 0.5 μm thick. As explained in the previous section, there is a real concern over the effect of the squeeze film.

To determine how long the gap closure takes we must set up a dynamic model. For simplicity, we will ignore dynamic variance in the stress of the membrane. Thus, the only forces acting on a given section of the membrane are the capacitive force, the pressure gradient force, and the squeeze film damping force. We will use a simple model for the squeeze film effect based on the inverse gap cubed equation given in the previous section. We make rough estimates of the L and W terms and apply the relationship. Therefore, we can only expect an order of magnitude result.

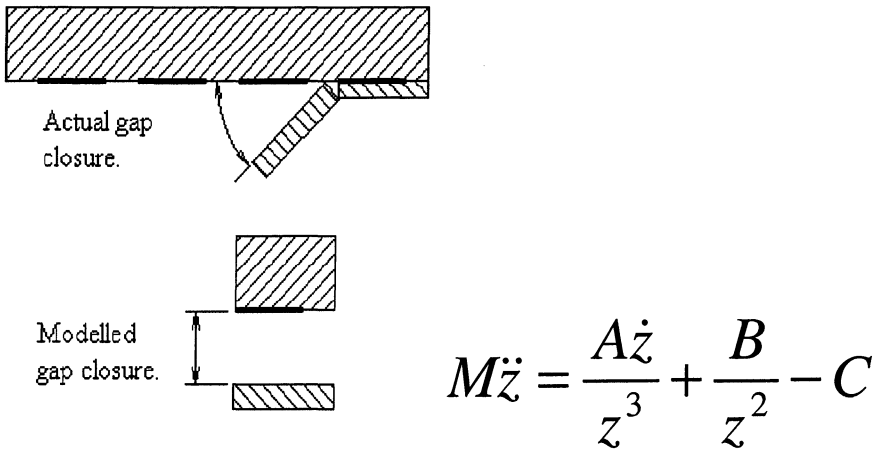

$$M\ddot{z} = \frac{A\dot{z}}{z^3} + \frac{B}{z^2} - C$$

Figure 7.1 Conceptual view of actual versus modeled gap closures.

A straightforward numerical model was built upon these three forces based on the z-direction force balance equation given in Figure 7.1. Note that z is the wall/membrane gap. In this equation, the left-hand side is, obviously, the inertia term while on the right

hand side we have the squeeze film damping term, the capacitive force term, and the pressure gradient term, respectively. A, B, and C are assumed to be time invariant, while M is the mass of the section of membrane in question. This happens to be an unstable system which behaves in two different ways depending on the initial conditions. If the initial gap is greater than a certain threshold value (equal to $\sqrt{B/C}$ for zero initial velocity) the gap will grow without bound. On the other hand, if the initial gap is inside that threshold, the gap will collapse faster than asymptotically. In other words, the gap will eventually close. It is easy to get the initial gap inside this threshold in our system due to the zipping action, so the only issue is whether the gap can close fast enough.

The time it takes for closure is related to the constants M, A, and B in a very complicated way which cannot be given by a simple expression. However, numerically, it has been found that this closure time is only a fraction of the time it takes for the wave to advance one electrode width for the geometries considered viable up to this point. Assuming a 100 μm electrode the time it takes to advance is given by:

$$t = \frac{100\mu m}{Tf} = \frac{.1mm}{(1.6mm)(827Hz)} = 75.6\mu\text{sec}$$

Figure 7.2 illustrates a nearly worst-case gap closure trajectory. Note that the ~7 μsec

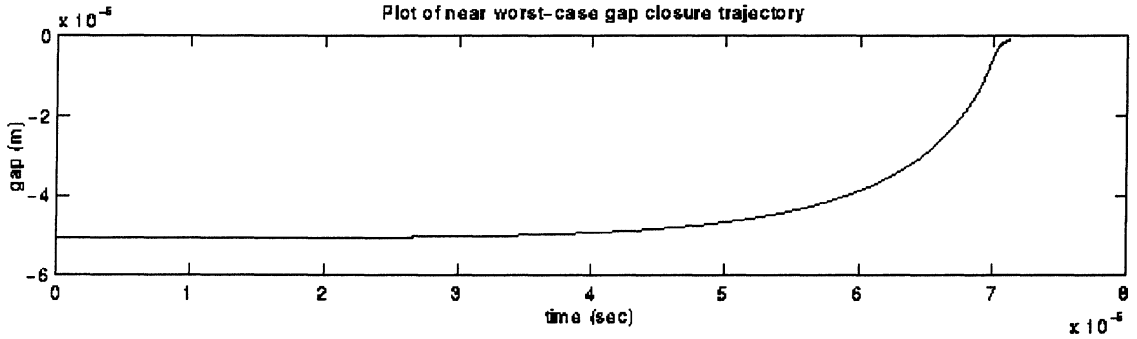

Figure 7.2 Near worst case gap closure trajectory calculated using simple model.

time to closure is indeed much smaller than 75.6 μsec even though the initial velocity is given as 0 and the initial position is very near the threshold level. In reality there will be a substantial initial velocity and the gap will start out far narrower.

The simple model of squeeze film damping used in this calculation has been used in the model of the beam system reported in Gupta and Senturia [9]. As can be seen in Figure 7.3, the model correctly predicts the gap closure time experimentally determined and predicted in that paper.

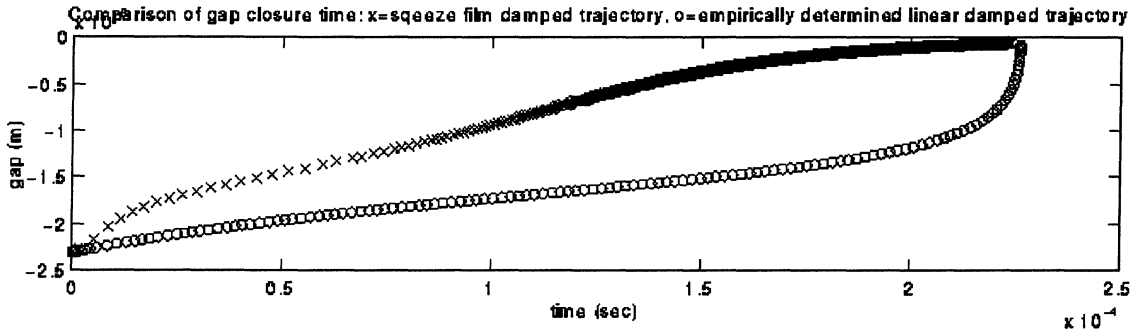

Figure 7.3 Comparison of gap closure time for simple model versus empirical model.

8. CONCLUSION

8.1 Summary

The goal of this document was to present and analyze a revolutionary new design for a compressor. The design was studied from a variety of standpoints ranging from energy balance to dynamics. Care was taken that whenever assumptions or approximations were used, they were conservative when compared to the true system.

The basic shape of the compressor channel was chosen in order to conform to the natural deformation of the diaphragm. The refrigerant specific numbers for the channel geometry were then found using an energy balance approach. Required work was equated to available energy, thus setting up constraints on the geometric parameters of the channel. With these constraints, an optimum geometry was selected, taking into account the desired flat compressor characteristics.

In addition, several major benefits of the design were examined. First, by taking a multistage approach to compression, the design avoids the problems associated with capacitance supported high pressure drops. Also, by using a continuous compression process from inlet to outlet, there is a smooth temperature gradient from one end of the compressor to the other. This has a twofold benefit. First, there are very small temperature differences between pockets, thus preventing deleterious heat transfer; and second it allows the hot end of the compressor to be isolated from the cool end so that beneficial heat transfer can take place from the hot (i.e. outlet) end. This second benefit was studied in detail. Other important benefits that were discussed were an easily adjustable flow rate, easily adjustable volume ratio, simplicity of control, simplicity of construction, and the fact that no valves are needed.

Possible problems with the design were also studied. The problems of device startup and electrode sealing, which are related to the fact that capacitor plates must be very close together in order to generate significant force, were addressed. Problems with

exposure of a free diaphragm edge to the flow was also examined. Detailed comparisons were made of the total available energy to total required work. Viscous energy dissipation was also studied. Finally, a dynamic analysis of the diaphragm motion was examined to determine whether the diaphragm could move fast enough to compress the refrigerant.

8.2 Results

The most important result of this analysis was that none of the possible problems identified appeared to be excessively difficult to resolve. Two different electrode 'zipping' modes were identified to be used for startup and electrode actuation. Using a simple design modification, it was found that no unsupported diaphragm edges needed to be exposed to refrigerant flow. Also, with a reasonable applied voltage, available energy was found to exceed required work. Viscous dissipation was shown to be insignificant to compressor operation, and diaphragm dynamics were found to be an order of magnitude faster than necessary. In addition, the design provides interesting possibilities that have not been available in prior compressor designs. These possibilities were identified in the previous section.

8.3 Future Work

The results of this analysis are very encouraging for the possible utility of the peristaltic compressor. However, all analysis performed in this paper is based on theory. No prototype was available to permit collection of empirical data. No matter how detailed the analysis, no analysis of a device can ever be complete without physical testing of the actual device. The analysis that has been presented lays a very strong foundation, though, on which a prototype might be constructed. When such a device is constructed, a number of tests should be performed. Electrode density (i.e. the number of electrodes per wavelength) should be varied and tested. The location at which heat transfer is permitted should also be studied. The device should be tested at a variety of operating frequencies and volume ratios as well. And finally, if possible, various

diaphragm materials should be studied. While the design of a peristaltic compressor presented in this document is by no means complete, this analysis makes pursuit of the construction of a working device seem like an extremely worthwhile endeavor.

APPENDIX A

Programs Developed in EES (Engineering Equation Solver) Version 4.644

Cpwk600a.EES

```
{This is an EES program listing for calculating the work required to
compress each pocket of the peristaltic compressor half a wavelength
forward using R134a.  The algorithm assumes no heat transfer until the
refrigerant is hotter than the wall of the compressor (i.e. insulated),
and thereafter it assumes heat transfer using a heat transfer
coefficient calculated for each pocket.}

function calcpow(p1,t1,f,Tw)

{This function takes the following inputs:

                  p1 = inlet pressure
                  t1 = inlet temperature
                  f  = operating frequency
                  Tw = Compressor wall temperature

It also assumes that the first column of the lookup table is a list of
all the pocket wall surface areas from inlet to outlet, while the
second column contains the corresponding pocket volume.  It then
outputs to the lookup table the corresponding pocket values for:

                  Column 3: pressure
                  Column 4: temperature
                  Column 5: work
                  Column 6: enthalpy
                  Column 7: entropy
}

{Calculation of pocket mass and mass flow}
rho1:=Density(R134a,P=p1,T=t1)
mdot:=2*rho1*Lookup(1,2)*f
m:=mdot/(2*f)

{Setting initial lookup table output values}
Lookup(1,3):=p1
Lookup(1,4):=t1
Lookup(1,6):=Enthalpy(R134a,T=t1,v=Lookup(1,2)/m)
Lookup(1,7):=Entropy(R134a,T=t1,v=Lookup(1,2)/m)

{initialize adiabatic loop}
i:=1
repeat

{calculate state variables}
ss:=Entropy(R134a,P=Lookup(i,3),v=Lookup(i,2)/m)
pp:=Pressure(R134a,v=Lookup(i+1,2)/m,s=ss)
TT:=Temperature(R134a,P=pp,v=Lookup(i+1,2)/m)

{output state variables and calculated work to lookup table}
j:=i+1
```

```
Lookup(j,3):=pp
Lookup(j,4):=TT
{work calculated using Pdv where P is taken as average pressure}
Lookup(i,5):=.5*(Lookup(i,3)+Lookup(i+1,3))*(Lookup(i,2)-Lookup(i+1,2))*1000
Lookup(j,6):=Enthalpy(R134a,T=Lookup(i+1,4),v=Lookup(i+1,2)/m)
Lookup(j,7):=Entropy(R134a,T=Lookup(i+1,4),v=Lookup(i+1,2)/m)

i:=i+1 {increment counter}

{exit loop if refrigerant temp > wall temp, or reach end of channel}
until(TT>Tw) OR (i>99)

IF (i>99) THEN GOTO 10 {skip heat transfer loop if at end of channel}

{start heat transfer loop}
repeat

{find refrigerant quality}
x:=Quality(R134a,P=Lookup(i,3),h=Lookup(i,6))

{if refrigerant is saturated vapor then find conductivity and specific
heat}
IF (abs(x)>1) THEN
k:=Conductivity(R134a,P=Lookup(i,3),T=Lookup(i,4))
cp:=Specheat(R134a,P=Lookup(i,3),T=Lookup(i,4))

{otherwise determine effective conductivity and specific heat using a
weighted average of saturated vapor and saturated liquid values where x
is the weighting}
ELSE
temp1:=Temperature(R134a,P=Lookup(i,3),x=1)+.1
temp0:=Temperature(R134a,P=Lookup(i,3),x=0)-.1
k1:=Conductivity(R134a,P=Lookup(i,3),T=temp1)
k0:=Conductivity(R134a,P=Lookup(i,3),T=temp0)
k:=x*k1+(1-x)*k0
cp1:=Specheat(R134a,P=Lookup(i,3),T=temp1)
cp0:=Specheat(R134a,P=Lookup(i,3),T=temp0)
cp:=x*cp1+(1-x)*cp0
ENDIF

{calculate state variables}
ss:=Entropy(R134a,P=Lookup(i,3),v=Lookup(i,2)/m)
pp:=Pressure(R134a,v=Lookup(i+1,2)/m,s=ss)
TT:=Temperature(R134a,P=pp,v=Lookup(i+1,2)/m)

j:=i+1
{determine heat transfer coefficient using h=Nu*k/Dh where Dh=hydraulic
diameter and Nu =~7.5 for this laminar flow}
h:=37500*k

{Compute the heat transfer corrected temperature where TT is adiabatic
temperature, so T=TT-dT where dT=Q/(mdot*cp) and Q=h*A*(T-Tw). Putting
these together we get TT-T=dT=h*A*(T-Tw)/(mdot*cp). Solving for T we
get T=(TT+b*Tw)/(1+b) where b=h*A/(mdot*cp)}
b:=h*Lookup(i+1,1)/(mdot*cp)
Lookup(j,4):=(TT+b*Tw)/(1+b)
```

```
{output other state variables and calculated work to lookup table}
Lookup(j,3):=Pressure(R134a,T=Lookup(i+1,4),v=Lookup(i+1,2)/m)
{work is Pdv again where P is average pressure}
Lookup(i,5):=.5*(Lookup(i,3)+Lookup(i+1,3))*(Lookup(i,2)-Lookup(i+1,2))*1000
Lookup(j,6):=Enthalpy(R134a,T=Lookup(i+1,4),v=Lookup(i+1,2)/m)
Lookup(j,7):=Entropy(R134a,T=Lookup(i+1,4),v=Lookup(i+1,2)/m)

i:=i+1 {increment counter}

until(i>99) {exit loop when end of channel reached}

10: calcpow:=1
end

{calculate work and all state variables in each compressor pocket given
a specific set of inlet conditions using the calcpow funtion}
a=calcpow(521,295,826.6,318)
```

```
{This is an EES program listing for calculating the work required to
compress each pocket of the peristaltic compressor half a wavelength
forward using R600a.  The algorithm assumes no heat transfer until the
refrigerant is hotter than the wall of the compressor (i.e. insulated),
and thereafter it assumes heat transfer using a heat transfer
coefficient calculated for each pocket.}

function calcpow(p1,t1,f,Tw)

{This function takes the following inputs:

                  p1 = inlet pressure
                  t1 = inlet temperature
                  f  = operating frequency
                  Tw = Compressor wall temperature

It also assumes that the first column of the lookup table is a list of
all the pocket wall surface areas from inlet to outlet, while the
second column contains the corresponding pocket volume.  It then
outputs to the lookup table the corresponding pocket values for:

                  Column 3: pressure
                  Column 4: temperature
                  Column 5: work
                  Column 6: enthalpy
                  Column 7: entropy
}

{Calculation of pocket mass and mass flow}
rho1:=Density(R600a,P=p1,T=t1)
mdot:=2*rho1*Lookup(1,2)*f
m:=mdot/(2*f)

{Setting initial lookup table output values}
Lookup(1,3):=p1
Lookup(1,4):=t1
Lookup(1,6):=Enthalpy(R600a,T=t1,v=Lookup(1,2)/m)
Lookup(1,7):=Entropy(R600a,T=t1,v=Lookup(1,2)/m)

{initialize adiabatic loop}
i:=1
repeat

{calculate state variables}
ss:=Entropy(R600a,P=Lookup(i,3),v=Lookup(i,2)/m)
pp:=Pressure(R600a,v=Lookup(i+1,2)/m,s=ss)
TT:=Temperature(R600a,P=pp,v=Lookup(i+1,2)/m)

{output state variables and calculated work to lookup table}
j:=i+1
Lookup(j,3):=pp
Lookup(j,4):=TT
{work calculated using Pdv where P is taken as average pressure}
Lookup(i,5):=.5*(Lookup(i,3)+Lookup(i+1,3))*(Lookup(i,2)-Lookup(i+1,2))*1000
Lookup(j,6):=Enthalpy(R600a,T=Lookup(i+1,4),v=Lookup(i+1,2)/m)
```

```
Lookup(j,7):=Entropy(R600a,T=Lookup(i+1,4),v=Lookup(i+1,2)/m)

i:=i+1 {increment counter}

{exit loop if refrigerant temp > wall temp, or reach end of channel}
until(TT>Tw) OR (i>49)

IF (i>49) THEN GOTO 10 {skip heat transfer loop if at end of channel}

{start heat transfer loop}
repeat

{find refrigerant quality}
x:=Quality(R600a,P=Lookup(i,3),h=Lookup(i,6))

{if refrigerant is saturated vapor then find conductivity and specific
heat}
IF (abs(x)>1) THEN
k:=Conductivity(R600a,P=Lookup(i,3),T=Lookup(i,4))
cp:=Specheat(R600a,P=Lookup(i,3),T=Lookup(i,4))

{otherwise determine effective conductivity and specific heat using a
weighted average of saturated vapor and saturated liquid values where x
is the weighting}
ELSE
temp1:=Temperature(R600a,P=Lookup(i,3),x=1)+.1
temp0:=Temperature(R600a,P=Lookup(i,3),x=0)-.1
k1:=Conductivity(R600a,P=Lookup(i,3),T=temp1)
k0:=Conductivity(R600a,P=Lookup(i,3),T=temp0)
k:=x*k1+(1-x)*k0
cp1:=Specheat(R600a,P=Lookup(i,3),T=temp1)
cp0:=Specheat(R600a,P=Lookup(i,3),T=temp0)
cp:=x*cp1+(1-x)*cp0
ENDIF

{calculate state variables}
ss:=Entropy(R600a,P=Lookup(i,3),v=Lookup(i,2)/m)
pp:=Pressure(R600a,v=Lookup(i+1,2)/m,s=ss)
TT:=Temperature(R600a,P=pp,v=Lookup(i+1,2)/m)

j:=i+1
{determine heat transfer coefficient using h=Nu*k/Dh where Dh=hydraulic
diameter and Nu =~7.5 for this laminar flow}
h:=37500*k

{Compute the heat transfer corrected temperature where TT is adiabatic
temperature, so T=TT-dT where dT=Q/(mdot*cp) and Q=h*A*(T-Tw). Putting
these together we get TT-T=dT=h*A*(T-Tw)/(mdot*cp). Solving for T we
get T=(TT+b*Tw)/(1+b) where b=h*A/(mdot*cp)}
b:=h*Lookup(i+1,1)/(mdot*cp)
Lookup(j,4):=(TT+b*Tw)/(1+b)

{output other state variables and calculated work to lookup table}
Lookup(j,3):=Pressure(R600a,T=Lookup(i+1,4),v=Lookup(i+1,2)/m)
{work is Pdv again where P is average pressure}
Lookup(i,5):=.5*(Lookup(i,3)+Lookup(i+1,3))*(Lookup(i,2)-Lookup(i+1,2))*1000
Lookup(j,6):=Enthalpy(R600a,T=Lookup(i+1,4),v=Lookup(i+1,2)/m)
```

```
Lookup(j,7):=Entropy(R600a,T=Lookup(i+1,4),v=Lookup(i+1,2)/m)

i:=i+1 {increment counter}

until(i>49) {exit loop when end of channel reached}

10: calcpow:=1
end

{calculate work and all state variables in each compressor pocket given
a specific set of inlet conditions using the calcpow funtion}
a=calcpow(276.4,Temperature(R600a,P=276.4,x=0.5)+1,826.6,318)
```

Visc600a.EES

```
{This EES program computes the pressure drop in the compressor
due to viscous dissipation using R600a, assuming a constant cross
sectional area that is an ellipse.}

{Input Parameters}
T_sat=20
DT_sup=5
T_comp_in=T_sat+DT_sup

{Average Width}
W=1.75E-02  {m}

{Average Height}
H=75E-06  {m}

L=4E-02  {m}
P_sat=PRESSURE(R600a,T=T_sat,x=0)
mu=VISCOSITY(R600a,T=T_comp_in,P=P_sat)
rho=DENSITY(R600a,T=T_comp_in,P=P_sat)

{for an ellipse of semi-major axis "a" and semi-minor axis "b"}
W=2*a; H=2*b

{area of ellipse}
Area=pi*a*b

{mass flow rate based on 3 W of heat dissipation and the latent
heat of evaporation of the refrigerant}
mdot=3E-03/(ENTHALPY(R600a,T=T_sat,x=1)-ENTHALPY(R600a,T=T_sat,x=0))

{volume flow rate in m^3/s}
Q=mdot/rho

{pgrad is the pressure gradient in Pa/m}
pgrad=(Q*(4*mu)/pi)*(a^2+b^2)/((a^3)*(b^3))

{Pressure drop across the compressor in Pa}
DELTAP=pgrad*L

{pressure drop in compressor as a percentage of the saturation
pressure at compressor entrance}
Perc=(DELTAP*1E-03/P_sat)*100
```

Visc134a.EES

```
{This EES program computes the pressure drop in the compressor
due to viscous dissipation using R134a, assuming a constant cross
sectional area that is an ellipse.}

{Input Parameters}
T_sat=20
DT_sup=5
T_comp_in=T_sat+DT_sup

{Average Width}
W=1.75E-02  {m}

{Average Height}
H=75E-06  {m}

L=4E-02  {m}
P_sat=PRESSURE(R134a,T=T_sat,x=0)
mu=VISCOSITY(R134a,T=T_comp_in,P=P_sat)
rho=DENSITY(R134a,T=T_comp_in,P=P_sat)

{for an ellipse of semi-major axis "a" and semi-minor axis "b"}
W=2*a; H=2*b

{area of ellipse}
Area=pi*a*b

{mass flow rate based on 3 W of heat dissipation and the latent
heat of evaporation of the refrigerant}
mdot=3E-03/(ENTHALPY(R134a,T=T_sat,x=1)-ENTHALPY(R134a,T=T_sat,x=0))

{volume flow rate in m^3/s}
Q=mdot/rho

{pgrad is the pressure gradient in Pa/m}
pgrad=(Q*(4*mu)/pi)*(a^2+b^2)/((a^3)*(b^3))

{Pressure drop across the compressor in Pa}
DELTAP=pgrad*L

{pressure drop in compressor as a percentage of the saturation
pressure at compressor entrance}
Perc=(DELTAP*1E-03/P_sat)*100
```

APPENDIX B

Programs Developed in Maple V Release 3.0 for Microsoft Windows

Peri1.ms

```
>! This is a Maple V program listing for calculating channel taper slope and
>! Operating frequency given geometric input parameters and the volumetric
>! Input/output ratio, R.
>
>! Input parameters
>! Half of channel width
>xmax:=10:
>
>! Channel length
>ymax:=40:
>
>! Number of wavelengths
>n:=25:
>
>! Amplitude
>a:=.05:
>
>! Volumetric input/output ratio
>R:=2.8313:
>
>! Inlet volumetric velocity
>v1dot:=1.75e3:
>
>! Wavelength calculation
>Lambda:=ymax/n:
>
>! Input and output volumes (see text)
>v1:=(16/15)*(a^2*xmax/mu)*(1-(1-(mu*Lambda/(2*a)))^(5/2)):
>v2:=(16/15)*(a^2*xmax/mu)*((1-mu*(ymax-(T/2))/a)^(5/2)-(1-mu*ymax/a)^(5/2)):
>
>! Solve for taper slope and operating frequency
>temp:=fsolve(v1/v2=R,mu=0..(a/ymax)):
>mu:=temp;
>f:=v1dot/(2*v1);
>restart:
>
```

```
>! This is a Maple V program listing for determining the lambda (see text)
>! Value which maximizes the allowed final electrode gap, d.
>
>! Input parameters
>! Permittivity of free space
>e0:=8.85e-12:
>
>! Dielectric constant
>k:=2:
>
>! Applied voltage
>V:=120:
>
>! Membrane elastic modulus
>E1:=12.13e9:
>
>! Poisson ratio of membrane
>nu:=.34:
>
>! Membrane thickness
>t:=2e-6:
>
>! Average pressure difference between pockets
>dp:=.01e6:
>
>! Channel amplitude
>a:=.05e-3:
>
>! Wavelength (note Lambda does not = lambda)
>Lambda:=1.6e-3:
>
>! See text for explanation of following parameters
>dx:=lambda*Lambda/2:
>alpha:=.5*(2*a/dx)^2:
>beta:=(1+3*alpha)/24:
>eta:=lambda*E1*t/(6*(1-nu^2)*dp*dx):
>gamma1:=eta*(3*beta+8*alpha^3*eta^2+sqrt(9*beta^2+48*alpha^3*beta*eta^2)):
>u:=gamma1^(1/3)+4*alpha^2*eta^2/gamma1^(1/3)+2*alpha*eta:
>
>! Calculation of strain and strain work
>epsilon:=lambda*(alpha+beta/u^2):
>Ws:=E1*epsilon^3*Lambda*t/(12*(1-nu^2)):
>
>! Electrode gap
>d:=e0*k*(Lambda/2-dx)*V^2/(Ws):
>
>! Plot of d vs lambda
>plot(1e6*d, lambda=0..1);
>
>! Solve for maximum and maximizing lambda value
>lambda:=fsolve(diff(d,lambda)=0,lambda,0.2..0.76);
>d:=e0*k*(T/2-dx)*V^2/(Ws);
>restart:
>
```

APPENDIX C

Functions and Scripts Developed in Matlab for Windows Version 4.2

Compress.m

```
function yp=compress(t,y)

% Compress is a function for use with the Runge-Kutta nonlinear
% ordinary differential equation solver matlab function of ode23
% the function is a first order dif-eq matrix form of the simple
% dynamic modelled shown in the text.  All paramters are given in
% the List of Symbols except that th is used for thickness rather
% than t so that t may be used for time.  Note that Lambda is
% not = lambda.

% specify all parameters
a=.05e-3;
lambda=.25;
Lambda=1.6e-3;
f=826.6;
rho=2000;
dp0=.01e6;
e0=8.854e-12;
k=2;
L=20e-3;
V=170;
mu=7.47e-6;
th=2e-6;

% calculate the pocket contact area
Ym=(1-lambda)*Lambda/2;

% find width of electrodes.
Dy=Ym/6;

% time to release
tf=Ym/(f*Lambda);

% give assumed linear pressure function
dp=dp0*(1-2*t/tf);

% specify equation parmeters
A=24*mu*L*dy^3/(pi^4);
B=e0*k*V^2*L*dy/2;
C=dp*L*dy;
M=rho*dy*L*th;

% first order dif-eq output
yp(1)=y(2);
yp(2)=(A/M)*y(2)/y(1)^3+(B/M)/y(1)^2-C/M;
```

Comprss2.m

```
function yp=comprss2(t,y)

% same as Compress except that dp is taken as constant

a=.05e-3;
lambda=.25;
T=1.6e-3;
f=826.6;
rho=2330;
dp0=.01e6;
e0=8.854e-12;
k=1;
L=.61e-3;
V=10;
mu=1.82e-5;
th=2.2e-6;
Ym=(1-lambda)*T/2;
dy=40e-6;
tf=Ym/(f*T);
A=56*mu*L*dy^3/pi^4;
B=e0*k^2*V^2*L*dy/2;
C=4.6;
M=rho*dy*L*th;
y0=-2.3e-6;

yp(1)=y(2);
yp(2)=(A/M)*y(2)/y(1)^3+(B/M)/y(1)^2-C*(y(1)-y0)/M;
```

Perchan2.m

```
function Z=perchan2(x,y,ampl,taper)

% Perchan2 takes the following inputs:
%           x = vector of values between -xmax and xmax
%           y = vector of values between 0 and ymax
%           ampl = maximum channel amplitude
%           taper = amplitude taper slope
%
% and it outputs a matrix which gives a representation of the
% channel shape.

% turn vectors into matrices
[X,Y]=meshgrid(x,y);

% channel shape calculation
A=ampl/max(x)^2;
R=1/(2*A);
Zo=R-ampl+taper*Y;
L=2*sqrt((R-Zo)/A);

% intitialize ouput to zero and then only set those values
% which are nonzero

Z=zeros(size(X));
a=abs(X)<L/2;
Z(a)=-Zo(a)+sqrt(R^2-X(a).^2);
```

```
function Z=permemb2(x,y,ampl,taper,per,n,lam,f,t)

% Permemb2 takes the following arguments:
%           x = vector of values between -xmax and xmax
%           y = vector of values between 0 and ymax
%           ampl = maximum channel amplitude
%           taper = amplitude taper slope
%           per = wavelength
%           n = number of pockets
%           lam = pocket slope parameter (see text)
%           f = frequency (optional)
%           t = time after compressor start
%
% and it outputs a matrix which represents the shape of the
% diaphragm membrane.

% determine number of arguments, and if <9 set f and t to 0
if nargin<9
f=0;
t=0;
end

% turn vectors into matrices
[X,Y]=meshgrid(x,y);

% calculate ripple envelope
Lam=max(lam)+(min(lam)-max(lam))*Y/(n*per);
b=1./Lam;
env=b.*sawtooth(2*pi*(Y/per+.25*(1-Lam)-f*t),.5);

% limit envelope to less than 1, and then make the output the
% product of the envelope and the channel shape
p=abs(env)>1;
env(p)=sign(env(p));
Z=env.*perchan2(x,y,ampl,taper);
```

Permem2a.m

```
function Z=permem2a(x,y,ampl,taper,T,n,lam,f,t)

% Permem2a is exactly the same as permemb2 except that
% the absolute value of the output is taken

if nargin<9
f=0;
t=0;
end

Z=abs(permemb2(x,y,ampl,taper,T,n,lam,f,t));
```

Volume.m

```
function vol = volume(fun,xmin,xmax,dx,ymin,ymax,dy,p1,p2,p3,p4,p5,p6,p7,p8)

% Volume calculates the volume of an arbitrary function of x and y that can
% take up to 8 additional parameters.  The arguments are as follows:
%
%                  xmin = minimum x value
%                  xmax = maximum x value
%                  dx = x increment
%                  ymin, ymax and dy similar to above for y
%                  p1 - p8 arbitrary additional parameters
%
% volume uses a simple trapezoidal rule to calculate volume

% find number of arguments
n=nargin;

% initiate x and y vectors
x=xmin:dx:xmax;
y=ymin:dy:ymax;

% set argument string to be (x,y, plus additional parameters
arg='(x,y';
if n>7
for I=1⊗n-7)
arg = [arg ',p' int2str(I)];
end
end

% evaluate funtion
Z=eval([fun arg ')']);

% calculate volume
a=trapz(y,Z);
vol = trapz(x,a);
```

Vola600a.m

```
% This matlab script file generates the volume and area data used for
% the EES program to calculate work with R600a as the refrigerant.
% The pocket volume calculations are based on Figure C.1 which shows
% a cross sectional view of one wavelength within the channel.  The
% surface area calculations simply take a rectangular approximation
% since the width of the channel varies very little over half a wavelenth.
% input parameters are the same as in previous programs
n=25;
a=.05e-3;
Lambda=1.6e-3;
xmax=.01;
V=150;
mu=6.349e-4;
f=826.6;
yy=Lambda*(0:49)/2+Lambda/4;

% use an empirically determined change in lambda for accuracy
lam=.12-2.3*yy;

% loop through entire channel length determining volume as shown in Figure C.1
for I=1:49
v1=(-1)^(I-1)*volume('permemb2',-.01,.01,.000125,(I-1)*Lambda/2+lam(I)
Lambda/4,iLambda/2+lam(i)Lambda/4,.000005,a,mu,Lambda,n,lam(I));
v2=volume('permem2a',-.01,.01,.000125,(I-1)*Lambda/2,
I*Lambda/2+lam(I)*Lambda/2,.000005,a,mu,Lambda,n,lam(I));
v3=volume('perchan2',-.01,.01,.000125,(I-1)*Lambda/2,
I*Lambda/2+lam(I)*Lambda/2,.000005,a,mu);
v(I)=2*v1-v2+v3;
end
v(50)=v(49)-(1-lam(50))*(v(48)-v(49));

% determine surface areas as a simple width times half wavelength
am=a-mu*yy;
L=2*xmax*sqrt(1-mu*yy/a);
area=L*Lambda/2;
```

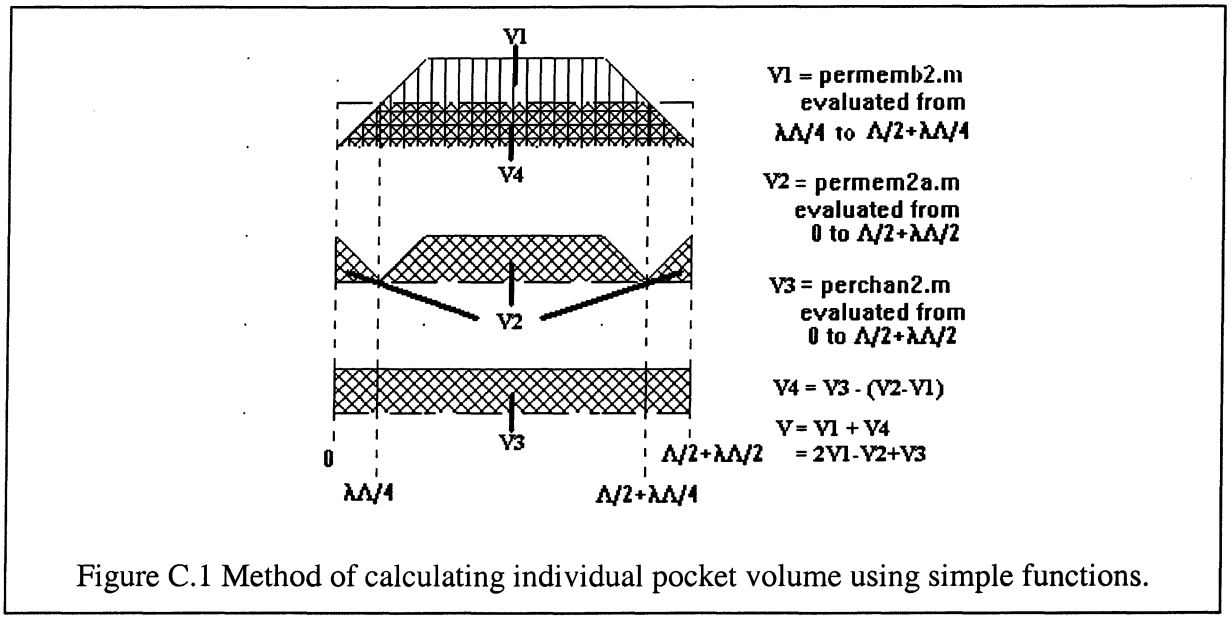

Figure C.1 Method of calculating individual pocket volume using simple functions.

Vola134a.m

```
% This matlab script file generates the volume and area data used for
% the EES program to calculate work with R134a as the refrigerant.
% The pocket volume calculations are based on Figure C.1 which shows
% a cross sectional view of one wavelength within the channel.  The
% surface area calculations simply take a rectangular approximation
% since the width of the channel varies very little over half a
% wavelenth.

% input parameters are the same as in previous programs
n=50;
a=.05e-3;
T=.8e-3;
xmax=.01;
V=150;
mu=6.403e-4;
f=865.8;
yy=T*(0:99)/2+T/4;

% use an empirically determined change in lambda for accuracy
lam=.75-15.75*yy;

% loop through entire channel length determining volume as shown in Figure C.1
for I=1:99
v1=(-1)^(I-1)*volume('permemb2',-.01,.01,.000125,(I-1)*T/2+lam(I)*T/4,
I*T/2+lam(I)*T/4,.000005,a,mu,T,n,lam(I));
v2=volume('permem2a',-.01,.01,.000125,(I-1)*T/2,I*T/2+lam(I)*T/2,
.000005,a,mu,T,n,lam(I));
v3=volume('perchan2',-.01,.01,.000125,(I-1)*T/2,
I*T/2+lam(I)*T/2,.000005,a,mu);
v(I)=2*v1-v2+v3;
end
v(100)=v(99)-(1-lam(100))*(v(98)-v(99));

% determine surface areas as a simple width times half wavelength
am=a-mu*yy;
L=2*xmax*sqrt(1-mu*yy/a);
area=L*T/2;
```

```
% This matlab script is used to take the data generated by the EES
% program for the calculation of work using R600a and plot it in a
% meaningful way.  It plots the compression path on a pressure vs
% enthalpy diagram to show what is happening during compression,
% and it plots a comparison of required work and available energy
% for each pocket to illustrate what kind of energy margin exists.
% The program prompts for a data file, which should be provided
% in the same format as the text saved version of the EES lookup
% table minus the first line (which is used for EES formatting).

% load in R600a vapor dome info
load r600a.txt

% data file prompt and loading code
inp=input('What is the data file name: ','s');
eval(['load ' inp '.txt'])
eval(['table = ' inp ';']);
w=table(1:49,5)';
p=1e3*table(:,3)';
v=table(:,2)';
area=table(:,1)';
temp=table(:,4)';
h=table(:,6)';
s=table(:,7)';

% input parameters.  Same as has been listed before.
N=25;
e0=8.85e-12;
a=.05e-3;
T=1.6e-3;
k=2;
V=150;
d=0.3e-6;
mu=6.349e-4;
yy=T*(0:49)/2+T/4;
lam=.12-2.3*yy;
am=a-mu*yy;

% work calculation which uses a simple averaging technique to
% account for the incomplete half wavelength of compression in
% the first and last pockets.
W1=([0 w]+[w 0])/2;

% similar technique used for pressure values
dp1=[0 p(2:50)-p(1:49)];
dp2=[dp1(2:50) 0];
dp=(dp1+dp2)/2;

% work calculation which accounts for the fact that the diaphragm
% must move through a pressure gradient. (see text)
w2=2*dp.*area.*am.*lam*T./sqrt((T*lam).^2+(4*am).^2);

% capacitive energy available
wc=e0*k*area*V^2/d;
```

```
% energy plotting code
plot(yy,w1+w2,'o',yy,wc,'x')
xlabel('Pocket position in channel (m)')
ylabel('Energy (J)')
title('Isobutane')
figure

% create vapor dome
twophase=[r600a(:,2) r600a(:,1)/1e3;r600a(50:-1:1,3) r600a(50:-1:1,1)/1e3];

% plot vapor dome and P-h data
semilogy(twophase(:,1),twophase(:,2),h,p/1e6,'.')
axis([0 1000 .01 10])
xlabel('Enthalpy [kJ/kg]')
ylabel('Pressure [Mpa]')
title('Isobutane')
grid

% optional code for plotting P-s diagram
%figure
%plot(s,temp,'+')
%axis([3 5.6 220 400])
%xlabel('Entropy [kJ/kg-K]')
%ylabel('Temperature [K]')
%title('Isobutane')
%grid
```

```
% This matlab script is used to take the data generated by the EES
% program for the calculation of work using R134a and plot it in a
% meaningful way.  It plots the compression path on a pressure vs
% enthalpy diagram to show what is happening during compression,
% and it plots a comparison of required work and available energy
% for each pocket to illustrate what kind of energy margin exists.
% The program prompts for a data file, which should be provided
% in the same format as the text saved version of the EES lookup
% table minus the first line (which is used for EES formatting).

% load in R134a vapor dome info
load r134a.txt

% data file prompt and loading code
inp=input('What is the data file name: ','s');
eval(['load ' inp '.txt'])
eval(['table = ' inp ';']);
w=table(1:99,5)';
p=1e3*table(:,3)';
v=table(:,2)';
area=table(:,1)';
temp=table(:,4)';
h=table(:,6)';
s=table(:,7)';

% input parameters.  Same as has been listed before.
N=50;
e0=8.85e-12;
a=.05e-3;
T=.8e-3;
k=2;
V=150;
d=0.3e-6;
mu=6.403e-4;
yy=T*(0:99)/2+T/4;
lam=.75-15.75*yy;
am=a-mu*yy;

% work calculation which uses a simple averaging technique to
% account for the incomplete half wavelength of compression in
% the first and last pockets.
W1=([0 w]+[w 0])/2;

% similar technique used for pressure values
dp1=[0 p(2:100)-p(1:99)];
dp2=[dp1(2:100) 0];
dp=(dp1+dp2)/2;

% work calculation which accounts for the fact that the diaphragm
% must move through a pressure gradient. (see text)
w2=2*dp.*area.*am.*lam*T./sqrt((T*lam).^2+(4*am).^2);

% capacitive energy available
```

```
wc=e0*k*area*V^2/d;

% energy plotting code
plot(yy,w1+w2,'o',yy,wc,'x')
xlabel('Pocket position in channel (m)')
ylabel('Energy (J)')
title('R134a')

% create vapor dome
figure
twophase=[r134a(:,2) r134a(:,1)/1e3;r134a(50:-1:1,3) r134a(50:-1:1,1)/1e3];

% plot vapor dome and P-h data
semilogy(twophase(:,1),twophase(:,2),h,p/1e6,'.')
axis([-50 400 .01 10])
xlabel('Enthalpy [kJ/kg]')
ylabel('Pressure [Mpa]')
title('R134a')
grid

% optional code for plotting P-s diagram
%figure
%plot(s,temp,'+')
%axis([3 5.6 220 400])
%xlabel('Entropy [kJ/kg-K]')
%ylabel('Temperature [K]')
%title('R134a')
%grid
```

APPENDIX D

Various Sample Data Files

Sample Lookup Table Data for Cpwk600a.EES

Row	Area [m^2]	Volume [m^3]	Pressure [kPa]	Temperature [K]	Power [W]	Enthalpy [kJ/kg]	Entropy [kJ/kg-K]
1	1.60E-05	1.06E-09	2.76E+02	2.95E+02	4.46E-06	7.09E+02	3.78E+00
2	1.59E-05	1.04E-09	2.81E+02	2.96E+02	4.53E-06	7.09E+02	3.78E+00
3	1.58E-05	1.03E-09	2.85E+02	2.96E+02	4.60E-06	7.10E+02	3.78E+00
4	1.57E-05	1.01E-09	2.90E+02	2.96E+02	4.59E-06	7.10E+02	3.78E+00
5	1.56E-05	9.93E-10	2.95E+02	2.97E+02	4.72E-06	7.11E+02	3.78E+00
6	1.56E-05	9.77E-10	3.00E+02	2.97E+02	4.77E-06	7.12E+02	3.78E+00
7	1.55E-05	9.62E-10	3.05E+02	2.98E+02	4.86E-06	7.12E+02	3.78E+00
8	1.54E-05	9.46E-10	3.10E+02	2.98E+02	4.81E-06	7.13E+02	3.78E+00
9	1.53E-05	9.30E-10	3.15E+02	2.99E+02	4.90E-06	7.14E+02	3.78E+00
10	1.52E-05	9.15E-10	3.21E+02	2.99E+02	4.91E-06	7.14E+02	3.78E+00
11	1.51E-05	9.00E-10	3.26E+02	3.00E+02	5.10E-06	7.15E+02	3.78E+00
12	1.50E-05	8.84E-10	3.32E+02	3.00E+02	5.09E-06	7.16E+02	3.78E+00
13	1.50E-05	8.69E-10	3.38E+02	3.01E+02	5.18E-06	7.16E+02	3.78E+00
14	1.49E-05	8.54E-10	3.44E+02	3.02E+02	5.28E-06	7.17E+02	3.78E+00
15	1.48E-05	8.39E-10	3.50E+02	3.02E+02	5.23E-06	7.18E+02	3.78E+00
16	1.47E-05	8.24E-10	3.57E+02	3.03E+02	5.29E-06	7.18E+02	3.78E+00
17	1.46E-05	8.09E-10	3.63E+02	3.03E+02	5.35E-06	7.19E+02	3.78E+00
18	1.45E-05	7.95E-10	3.70E+02	3.04E+02	5.57E-06	7.20E+02	3.78E+00
19	1.44E-05	7.80E-10	3.77E+02	3.04E+02	5.56E-06	7.21E+02	3.78E+00
20	1.43E-05	7.65E-10	3.85E+02	3.05E+02	5.67E-06	7.21E+02	3.78E+00
21	1.42E-05	7.51E-10	3.92E+02	3.05E+02	5.74E-06	7.22E+02	3.78E+00
22	1.42E-05	7.36E-10	4.00E+02	3.06E+02	5.69E-06	7.23E+02	3.78E+00
23	1.41E-05	7.22E-10	4.08E+02	3.07E+02	5.81E-06	7.24E+02	3.78E+00
24	1.40E-05	7.08E-10	4.16E+02	3.07E+02	5.92E-06	7.24E+02	3.78E+00
25	1.39E-05	6.94E-10	4.24E+02	3.08E+02	6.04E-06	7.25E+02	3.78E+00
26	1.38E-05	6.80E-10	4.33E+02	3.09E+02	6.13E-06	7.26E+02	3.78E+00
27	1.37E-05	6.66E-10	4.42E+02	3.09E+02	6.21E-06	7.27E+02	3.78E+00
28	1.36E-05	6.52E-10	4.52E+02	3.10E+02	6.30E-06	7.28E+02	3.78E+00
29	1.35E-05	6.38E-10	4.61E+02	3.11E+02	6.29E-06	7.28E+02	3.78E+00
30	1.34E-05	6.24E-10	4.71E+02	3.11E+02	6.33E-06	7.29E+02	3.78E+00
31	1.33E-05	6.11E-10	4.81E+02	3.12E+02	6.62E-06	7.30E+02	3.78E+00
32	1.32E-05	5.98E-10	4.92E+02	3.13E+02	6.67E-06	7.31E+02	3.78E+00
33	1.31E-05	5.84E-10	5.03E+02	3.13E+02	6.77E-06	7.32E+02	3.78E+00
34	1.30E-05	5.71E-10	5.15E+02	3.14E+02	6.82E-06	7.33E+02	3.78E+00
35	1.29E-05	5.58E-10	5.27E+02	3.15E+02	7.04E-06	7.34E+02	3.78E+00
36	1.28E-05	5.45E-10	5.39E+02	3.15E+02	6.93E-06	7.34E+02	3.78E+00
37	1.27E-05	5.32E-10	5.52E+02	3.16E+02	7.09E-06	7.35E+02	3.78E+00
38	1.26E-05	5.19E-10	5.65E+02	3.17E+02	7.32E-06	7.36E+02	3.78E+00
39	1.25E-05	5.06E-10	5.79E+02	3.18E+02	7.44E-06	7.37E+02	3.78E+00
40	1.24E-05	4.94E-10	5.93E+02	3.19E+02	7.51E-06	7.38E+02	3.78E+00
41	1.23E-05	4.81E-10	5.98E+02	3.18E+02	7.54E-06	7.33E+02	3.76E+00
42	1.22E-05	4.68E-10	5.98E+02	3.18E+02	7.24E-06	7.25E+02	3.74E+00
43	1.21E-05	4.56E-10	5.98E+02	3.18E+02	7.24E-06	7.17E+02	3.71E+00
44	1.20E-05	4.44E-10	5.98E+02	3.18E+02	7.06E-06	7.10E+02	3.69E+00

45	1.18E-05	4.32E-10	5.98E+02	3.18E+02	7.30E-06	7.02E+02	3.67E+00
46	1.17E-05	4.20E-10	5.98E+02	3.18E+02	7.12E-06	6.95E+02	3.64E+00
47	1.16E-05	4.08E-10	5.98E+02	3.18E+02	7.06E-06	6.87E+02	3.62E+00
48	1.15E-05	3.97E-10	5.98E+02	3.18E+02	7.12E-06	6.80E+02	3.60E+00
49	1.14E-05	3.85E-10	5.98E+02	3.18E+02	6.94E-06	6.72E+02	3.57E+00
50	1.13E-05	3.73E-10	5.98E+02	3.18E+02	0.00E+00	6.65E+02	3.55E+00

Sample Lookup Table Data for Cpwk134a.EES

Row	Area [m^2]	Volume [m^3]	Pressure [kPa]	Temperature [K]	Power [W]	Enthalpy [kJ/kg]	Entropy [kJ/kg-K]
1	7.99E-06	5.30E-10	5.21E+02	2.95E+02	2.15E-06	2.61E+02	9.24E-01
2	7.97E-06	5.26E-10	5.25E+02	2.95E+02	2.16E-06	2.61E+02	9.24E-01
3	7.95E-06	5.22E-10	5.30E+02	2.96E+02	2.13E-06	2.61E+02	9.24E-01
4	7.93E-06	5.18E-10	5.34E+02	2.96E+02	2.14E-06	2.61E+02	9.24E-01
5	7.91E-06	5.14E-10	5.38E+02	2.96E+02	2.22E-06	2.61E+02	9.24E-01
6	7.89E-06	5.09E-10	5.43E+02	2.96E+02	2.18E-06	2.62E+02	9.24E-01
7	7.87E-06	5.05E-10	5.47E+02	2.97E+02	2.14E-06	2.62E+02	9.24E-01
8	7.85E-06	5.02E-10	5.51E+02	2.97E+02	2.27E-06	2.62E+02	9.24E-01
9	7.82E-06	4.97E-10	5.56E+02	2.97E+02	2.23E-06	2.62E+02	9.24E-01
10	7.80E-06	4.93E-10	5.61E+02	2.98E+02	2.25E-06	2.62E+02	9.24E-01
11	7.78E-06	4.89E-10	5.65E+02	2.98E+02	2.21E-06	2.62E+02	9.24E-01
12	7.76E-06	4.86E-10	5.70E+02	2.98E+02	2.29E-06	2.63E+02	9.24E-01
13	7.74E-06	4.82E-10	5.75E+02	2.99E+02	2.25E-06	2.63E+02	9.24E-01
14	7.72E-06	4.78E-10	5.80E+02	2.99E+02	2.33E-06	2.63E+02	9.24E-01
15	7.70E-06	4.74E-10	5.85E+02	2.99E+02	2.23E-06	2.63E+02	9.24E-01
16	7.68E-06	4.70E-10	5.90E+02	2.99E+02	2.37E-06	2.63E+02	9.24E-01
17	7.65E-06	4.66E-10	5.95E+02	3.00E+02	2.33E-06	2.63E+02	9.24E-01
18	7.63E-06	4.62E-10	6.00E+02	3.00E+02	2.35E-06	2.64E+02	9.24E-01
19	7.61E-06	4.58E-10	6.05E+02	3.00E+02	2.31E-06	2.64E+02	9.24E-01
20	7.59E-06	4.54E-10	6.11E+02	3.01E+02	2.39E-06	2.64E+02	9.24E-01
21	7.57E-06	4.50E-10	6.16E+02	3.01E+02	2.41E-06	2.64E+02	9.24E-01
22	7.55E-06	4.46E-10	6.22E+02	3.01E+02	2.37E-06	2.64E+02	9.24E-01
23	7.53E-06	4.43E-10	6.27E+02	3.02E+02	2.39E-06	2.65E+02	9.24E-01
24	7.50E-06	4.39E-10	6.33E+02	3.02E+02	2.48E-06	2.65E+02	9.24E-01
25	7.48E-06	4.35E-10	6.38E+02	3.02E+02	2.44E-06	2.65E+02	9.24E-01
26	7.46E-06	4.31E-10	6.44E+02	3.03E+02	2.46E-06	2.65E+02	9.24E-01
27	7.44E-06	4.27E-10	6.50E+02	3.03E+02	2.42E-06	2.65E+02	9.24E-01
28	7.42E-06	4.24E-10	6.56E+02	3.03E+02	2.57E-06	2.66E+02	9.24E-01
29	7.39E-06	4.20E-10	6.62E+02	3.04E+02	2.46E-06	2.66E+02	9.24E-01
30	7.37E-06	4.16E-10	6.68E+02	3.04E+02	2.55E-06	2.66E+02	9.24E-01
31	7.35E-06	4.12E-10	6.74E+02	3.04E+02	2.51E-06	2.66E+02	9.24E-01
32	7.33E-06	4.09E-10	6.81E+02	3.05E+02	2.60E-06	2.66E+02	9.24E-01
33	7.30E-06	4.05E-10	6.87E+02	3.05E+02	2.55E-06	2.67E+02	9.24E-01
34	7.28E-06	4.01E-10	6.93E+02	3.05E+02	2.58E-06	2.67E+02	9.24E-01
35	7.26E-06	3.97E-10	7.00E+02	3.06E+02	2.53E-06	2.67E+02	9.24E-01
36	7.24E-06	3.94E-10	7.07E+02	3.06E+02	2.70E-06	2.67E+02	9.24E-01
37	7.21E-06	3.90E-10	7.14E+02	3.06E+02	2.65E-06	2.67E+02	9.24E-01
38	7.19E-06	3.86E-10	7.20E+02	3.07E+02	2.61E-06	2.68E+02	9.24E-01
39	7.17E-06	3.83E-10	7.27E+02	3.07E+02	2.63E-06	2.68E+02	9.24E-01
40	7.15E-06	3.79E-10	7.34E+02	3.08E+02	2.73E-06	2.68E+02	9.24E-01
41	7.12E-06	3.75E-10	7.42E+02	3.08E+02	2.76E-06	2.68E+02	9.24E-01
42	7.10E-06	3.72E-10	7.49E+02	3.08E+02	2.63E-06	2.68E+02	9.24E-01
43	7.08E-06	3.68E-10	7.56E+02	3.09E+02	2.74E-06	2.69E+02	9.24E-01
44	7.05E-06	3.65E-10	7.64E+02	3.09E+02	2.76E-06	2.69E+02	9.24E-01
45	7.03E-06	3.61E-10	7.72E+02	3.09E+02	2.87E-06	2.69E+02	9.24E-01
46	7.01E-06	3.57E-10	7.80E+02	3.10E+02	2.74E-06	2.69E+02	9.24E-01
47	6.98E-06	3.54E-10	7.87E+02	3.10E+02	2.77E-06	2.69E+02	9.24E-01
48	6.96E-06	3.50E-10	7.95E+02	3.11E+02	2.88E-06	2.70E+02	9.24E-01

49	6.94E-06	3.47E-10	8.04E+02	3.11E+02	2.91E-06	2.70E+02	9.24E-01
50	6.91E-06	3.43E-10	8.12E+02	3.11E+02	2.86E-06	2.70E+02	9.24E-01
51	6.89E-06	3.40E-10	8.21E+02	3.12E+02	2.80E-06	2.70E+02	9.24E-01
52	6.86E-06	3.36E-10	8.29E+02	3.12E+02	2.92E-06	2.71E+02	9.24E-01
53	6.84E-06	3.33E-10	8.38E+02	3.13E+02	3.03E-06	2.71E+02	9.24E-01
54	6.82E-06	3.29E-10	8.47E+02	3.13E+02	2.89E-06	2.71E+02	9.24E-01
55	6.79E-06	3.26E-10	8.56E+02	3.13E+02	2.92E-06	2.71E+02	9.24E-01
56	6.77E-06	3.22E-10	8.65E+02	3.14E+02	3.04E-06	2.71E+02	9.24E-01
57	6.74E-06	3.19E-10	8.74E+02	3.14E+02	3.08E-06	2.72E+02	9.24E-01
58	6.72E-06	3.15E-10	8.84E+02	3.15E+02	3.02E-06	2.72E+02	9.24E-01
59	6.70E-06	3.12E-10	8.93E+02	3.15E+02	2.96E-06	2.72E+02	9.24E-01
60	6.67E-06	3.09E-10	9.03E+02	3.15E+02	3.18E-06	2.72E+02	9.24E-01
61	6.65E-06	3.05E-10	9.13E+02	3.16E+02	3.12E-06	2.73E+02	9.24E-01
62	6.62E-06	3.02E-10	9.23E+02	3.16E+02	3.06E-06	2.73E+02	9.24E-01
63	6.60E-06	2.98E-10	9.34E+02	3.17E+02	3.19E-06	2.73E+02	9.24E-01
64	6.57E-06	2.95E-10	9.44E+02	3.17E+02	3.13E-06	2.73E+02	9.24E-01
65	6.55E-06	2.92E-10	9.55E+02	3.18E+02	3.36E-06	2.74E+02	9.24E-01
66	6.52E-06	2.88E-10	9.66E+02	3.18E+02	3.11E-06	2.74E+02	9.24E-01
67	6.50E-06	2.85E-10	9.75E+02	3.18E+02	3.23E-06	2.74E+02	9.23E-01
68	6.47E-06	2.82E-10	9.84E+02	3.18E+02	3.26E-06	2.73E+02	9.21E-01
69	6.45E-06	2.78E-10	9.93E+02	3.18E+02	3.39E-06	2.73E+02	9.20E-01
70	6.42E-06	2.75E-10	1.00E+03	3.18E+02	3.22E-06	2.73E+02	9.19E-01
71	6.39E-06	2.72E-10	1.01E+03	3.18E+02	3.25E-06	2.73E+02	9.18E-01
72	6.37E-06	2.69E-10	1.02E+03	3.18E+02	3.39E-06	2.72E+02	9.16E-01
73	6.34E-06	2.65E-10	1.03E+03	3.18E+02	3.42E-06	2.72E+02	9.15E-01
74	6.32E-06	2.62E-10	1.04E+03	3.18E+02	3.24E-06	2.72E+02	9.13E-01
75	6.29E-06	2.59E-10	1.05E+03	3.18E+02	3.38E-06	2.72E+02	9.12E-01
76	6.27E-06	2.56E-10	1.06E+03	3.18E+02	3.41E-06	2.71E+02	9.11E-01
77	6.24E-06	2.52E-10	1.07E+03	3.18E+02	3.55E-06	2.71E+02	9.09E-01
78	6.21E-06	2.49E-10	1.08E+03	3.18E+02	3.26E-06	2.71E+02	9.08E-01
79	6.19E-06	2.46E-10	1.09E+03	3.18E+02	3.51E-06	2.71E+02	9.06E-01
80	6.16E-06	2.43E-10	1.10E+03	3.18E+02	3.43E-06	2.70E+02	9.05E-01
81	6.13E-06	2.40E-10	1.11E+03	3.18E+02	3.69E-06	2.70E+02	9.03E-01
82	6.11E-06	2.37E-10	1.12E+03	3.18E+02	3.39E-06	2.70E+02	9.02E-01
83	6.08E-06	2.34E-10	1.13E+03	3.18E+02	3.42E-06	2.70E+02	9.00E-01
84	6.05E-06	2.31E-10	1.14E+03	3.18E+02	3.68E-06	2.69E+02	8.99E-01
85	6.03E-06	2.27E-10	1.16E+03	3.18E+02	3.58E-06	2.69E+02	8.97E-01
86	6.00E-06	2.24E-10	1.16E+03	3.18E+02	3.47E-06	2.67E+02	8.90E-01
87	5.97E-06	2.21E-10	1.16E+03	3.18E+02	3.47E-06	2.64E+02	8.83E-01
88	5.94E-06	2.18E-10	1.16E+03	3.18E+02	3.58E-06	2.62E+02	8.76E-01
89	5.92E-06	2.15E-10	1.16E+03	3.18E+02	3.58E-06	2.60E+02	8.69E-01
90	5.89E-06	2.12E-10	1.16E+03	3.18E+02	3.24E-06	2.58E+02	8.62E-01
91	5.86E-06	2.09E-10	1.16E+03	3.18E+02	3.47E-06	2.56E+02	8.56E-01
92	5.83E-06	2.06E-10	1.16E+03	3.18E+02	3.47E-06	2.54E+02	8.49E-01
93	5.80E-06	2.03E-10	1.16E+03	3.18E+02	3.58E-06	2.51E+02	8.42E-01
94	5.78E-06	2.00E-10	1.16E+03	3.18E+02	3.24E-06	2.49E+02	8.35E-01
95	5.75E-06	1.97E-10	1.16E+03	3.18E+02	3.35E-06	2.47E+02	8.29E-01
96	5.72E-06	1.94E-10	1.16E+03	3.18E+02	3.47E-06	2.45E+02	8.22E-01
97	5.69E-06	1.91E-10	1.16E+03	3.18E+02	3.47E-06	2.43E+02	8.15E-01
98	5.66E-06	1.88E-10	1.16E+03	3.18E+02	3.12E-06	2.41E+02	8.08E-01
99	5.63E-06	1.86E-10	1.16E+03	3.18E+02	2.77E-06	2.39E+02	8.02E-01
100	5.60E-06	1.83E-10	1.16E+03	3.18E+02	0.00E+00	2.37E+02	7.97E-01

Sample Input Data File for wrk600a.m

1.596E-0005	1.057E-0009	2.764E+0002	2.950E+0002	4.457E-0006	7.085E+0002	3.781E+0000
1.588E-0005	1.041E-0009	2.808E+0002	2.955E+0002	4.529E-0006	7.091E+0002	3.781E+0000
1.580E-0005	1.025E-0009	2.853E+0002	2.959E+0002	4.602E-0006	7.097E+0002	3.781E+0000
1.571E-0005	1.009E-0009	2.900E+0002	2.964E+0002	4.589E-0006	7.103E+0002	3.781E+0000
1.563E-0005	9.933E-0010	2.947E+0002	2.969E+0002	4.724E-0006	7.110E+0002	3.781E+0000
1.555E-0005	9.774E-0010	2.996E+0002	2.974E+0002	4.774E-0006	7.116E+0002	3.781E+0000
1.546E-0005	9.616E-0010	3.047E+0002	2.979E+0002	4.855E-0006	7.123E+0002	3.781E+0000
1.538E-0005	9.458E-0010	3.099E+0002	2.984E+0002	4.812E-0006	7.129E+0002	3.781E+0000
1.529E-0005	9.304E-0010	3.151E+0002	2.989E+0002	4.895E-0006	7.136E+0002	3.781E+0000
1.521E-0005	9.150E-0010	3.206E+0002	2.994E+0002	4.914E-0006	7.142E+0002	3.781E+0000
1.512E-0005	8.998E-0010	3.261E+0002	2.999E+0002	5.100E-0006	7.149E+0002	3.781E+0000
1.504E-0005	8.843E-0010	3.319E+0002	3.004E+0002	5.090E-0006	7.156E+0002	3.781E+0000
1.495E-0005	8.691E-0010	3.378E+0002	3.009E+0002	5.182E-0006	7.163E+0002	3.781E+0000
1.486E-0005	8.539E-0010	3.440E+0002	3.015E+0002	5.276E-0006	7.170E+0002	3.781E+0000
1.477E-0005	8.387E-0010	3.503E+0002	3.020E+0002	5.232E-0006	7.177E+0002	3.781E+0000
1.469E-0005	8.239E-0010	3.567E+0002	3.026E+0002	5.292E-0006	7.184E+0002	3.781E+0000
1.460E-0005	8.092E-0010	3.633E+0002	3.031E+0002	5.353E-0006	7.191E+0002	3.781E+0000
1.451E-0005	7.946E-0010	3.700E+0002	3.037E+0002	5.567E-0006	7.198E+0002	3.781E+0000
1.442E-0005	7.797E-0010	3.772E+0002	3.043E+0002	5.560E-0006	7.205E+0002	3.781E+0000
1.433E-0005	7.651E-0010	3.845E+0002	3.048E+0002	5.668E-0006	7.213E+0002	3.781E+0000
1.424E-0005	7.505E-0010	3.920E+0002	3.054E+0002	5.740E-0006	7.220E+0002	3.781E+0000
1.415E-0005	7.360E-0010	3.998E+0002	3.060E+0002	5.692E-0006	7.228E+0002	3.781E+0000
1.405E-0005	7.219E-0010	4.076E+0002	3.066E+0002	5.805E-0006	7.235E+0002	3.781E+0000
1.396E-0005	7.078E-0010	4.158E+0002	3.072E+0002	5.922E-0006	7.243E+0002	3.781E+0000
1.387E-0005	6.937E-0010	4.242E+0002	3.079E+0002	6.044E-0006	7.251E+0002	3.781E+0000
1.377E-0005	6.796E-0010	4.331E+0002	3.085E+0002	6.126E-0006	7.259E+0002	3.781E+0000
1.368E-0005	6.656E-0010	4.421E+0002	3.091E+0002	6.211E-0006	7.267E+0002	3.781E+0000
1.358E-0005	6.517E-0010	4.515E+0002	3.098E+0002	6.298E-0006	7.275E+0002	3.781E+0000
1.349E-0005	6.379E-0010	4.613E+0002	3.105E+0002	6.294E-0006	7.283E+0002	3.781E+0000
1.339E-0005	6.244E-0010	4.712E+0002	3.111E+0002	6.334E-0006	7.292E+0002	3.781E+0000
1.329E-0005	6.111E-0010	4.813E+0002	3.118E+0002	6.620E-0006	7.300E+0002	3.781E+0000
1.319E-0005	5.975E-0010	4.922E+0002	3.125E+0002	6.670E-0006	7.309E+0002	3.781E+0000
1.310E-0005	5.841E-0010	5.033E+0002	3.132E+0002	6.771E-0006	7.317E+0002	3.781E+0000
1.300E-0005	5.708E-0010	5.148E+0002	3.139E+0002	6.822E-0006	7.326E+0002	3.781E+0000
1.289E-0005	5.577E-0010	5.267E+0002	3.147E+0002	7.035E-0006	7.335E+0002	3.781E+0000
1.279E-0005	5.445E-0010	5.392E+0002	3.154E+0002	6.928E-0006	7.344E+0002	3.781E+0000
1.269E-0005	5.318E-0010	5.518E+0002	3.161E+0002	7.092E-0006	7.353E+0002	3.781E+0000
1.259E-0005	5.191E-0010	5.650E+0002	3.169E+0002	7.320E-0006	7.362E+0002	3.781E+0000
1.249E-0005	5.063E-0010	5.788E+0002	3.177E+0002	7.443E-0006	7.371E+0002	3.781E+0000
1.238E-0005	4.936E-0010	5.933E+0002	3.185E+0002	7.506E-0006	7.381E+0002	3.781E+0000
1.228E-0005	4.810E-0010	5.981E+0002	3.180E+0002	7.536E-0006	7.328E+0002	3.763E+0000
1.217E-0005	4.684E-0010	5.981E+0002	3.180E+0002	7.237E-0006	7.249E+0002	3.738E+0000
1.206E-0005	4.563E-0010	5.981E+0002	3.180E+0002	7.237E-0006	7.173E+0002	3.714E+0000
1.195E-0005	4.442E-0010	5.981E+0002	3.180E+0002	7.057E-0006	7.097E+0002	3.690E+0000
1.184E-0005	4.324E-0010	5.981E+0002	3.180E+0002	7.297E-0006	7.022E+0002	3.667E+0000
1.173E-0005	4.202E-0010	5.981E+0002	3.180E+0002	7.117E-0006	6.946E+0002	3.643E+0000
1.162E-0005	4.083E-0010	5.981E+0002	3.180E+0002	7.057E-0006	6.871E+0002	3.619E+0000
1.151E-0005	3.965E-0010	5.981E+0002	3.180E+0002	7.117E-0006	6.797E+0002	3.596E+0000
1.140E-0005	3.846E-0010	5.981E+0002	3.180E+0002	6.938E-0006	6.722E+0002	3.573E+0000
1.128E-0005	3.730E-0010	5.981E+0002	3.180E+0002	0.000E+0000	6.649E+0002	3.550E+0000

Sample Input Data File for wrk600a.m

7.990E-0006	5.297E-0010	5.210E+0002	2.950E+0002	2.145E-0006	2.606E+0002	9.240E-0001
7.969E-0006	5.256E-0010	5.252E+0002	2.953E+0002	2.162E-0006	2.608E+0002	9.240E-0001
7.949E-0006	5.215E-0010	5.295E+0002	2.956E+0002	2.126E-0006	2.610E+0002	9.240E-0001
7.928E-0006	5.175E-0010	5.337E+0002	2.959E+0002	2.144E-0006	2.611E+0002	9.240E-0001
7.907E-0006	5.135E-0010	5.380E+0002	2.961E+0002	2.215E-0006	2.613E+0002	9.240E-0001
7.887E-0006	5.094E-0010	5.425E+0002	2.964E+0002	2.179E-0006	2.615E+0002	9.240E-0001
7.866E-0006	5.054E-0010	5.470E+0002	2.967E+0002	2.142E-0006	2.617E+0002	9.240E-0001
7.845E-0006	5.015E-0010	5.513E+0002	2.970E+0002	2.270E-0006	2.618E+0002	9.240E-0001
7.824E-0006	4.974E-0010	5.560E+0002	2.973E+0002	2.233E-0006	2.620E+0002	9.240E-0001
7.803E-0006	4.934E-0010	5.607E+0002	2.976E+0002	2.252E-0006	2.622E+0002	9.240E-0001
7.782E-0006	4.894E-0010	5.654E+0002	2.979E+0002	2.214E-0006	2.624E+0002	9.240E-0001
7.761E-0006	4.855E-0010	5.701E+0002	2.982E+0002	2.290E-0006	2.625E+0002	9.240E-0001
7.740E-0006	4.815E-0010	5.750E+0002	2.985E+0002	2.252E-0006	2.627E+0002	9.240E-0001
7.718E-0006	4.776E-0010	5.798E+0002	2.988E+0002	2.329E-0006	2.629E+0002	9.240E-0001
7.697E-0006	4.736E-0010	5.849E+0002	2.991E+0002	2.232E-0006	2.631E+0002	9.240E-0001
7.676E-0006	4.698E-0010	5.897E+0002	2.994E+0002	2.369E-0006	2.633E+0002	9.240E-0001
7.654E-0006	4.658E-0010	5.949E+0002	2.997E+0002	2.330E-0006	2.634E+0002	9.240E-0001
7.633E-0006	4.619E-0010	6.001E+0002	3.000E+0002	2.351E-0006	2.636E+0002	9.240E-0001
7.612E-0006	4.580E-0010	6.054E+0002	3.004E+0002	2.310E-0006	2.638E+0002	9.240E-0001
7.590E-0006	4.542E-0010	6.106E+0002	3.007E+0002	2.392E-0006	2.640E+0002	9.240E-0001
7.568E-0006	4.503E-0010	6.160E+0002	3.010E+0002	2.413E-0006	2.642E+0002	9.240E-0001
7.547E-0006	4.464E-0010	6.215E+0002	3.013E+0002	2.372E-0006	2.644E+0002	9.240E-0001
7.525E-0006	4.426E-0010	6.270E+0002	3.016E+0002	2.393E-0006	2.645E+0002	9.240E-0001
7.503E-0006	4.388E-0010	6.325E+0002	3.020E+0002	2.478E-0006	2.647E+0002	9.240E-0001
7.481E-0006	4.349E-0010	6.383E+0002	3.023E+0002	2.437E-0006	2.649E+0002	9.240E-0001
7.459E-0006	4.311E-0010	6.441E+0002	3.026E+0002	2.459E-0006	2.651E+0002	9.240E-0001
7.437E-0006	4.273E-0010	6.499E+0002	3.030E+0002	2.416E-0006	2.653E+0002	9.240E-0001
7.415E-0006	4.236E-0010	6.557E+0002	3.033E+0002	2.570E-0006	2.655E+0002	9.240E-0001
7.393E-0006	4.197E-0010	6.620E+0002	3.036E+0002	2.460E-0006	2.657E+0002	9.240E-0001
7.371E-0006	4.160E-0010	6.680E+0002	3.040E+0002	2.550E-0006	2.659E+0002	9.240E-0001
7.349E-0006	4.122E-0010	6.743E+0002	3.043E+0002	2.506E-0006	2.661E+0002	9.240E-0001
7.326E-0006	4.085E-0010	6.805E+0002	3.046E+0002	2.598E-0006	2.663E+0002	9.240E-0001
7.304E-0006	4.047E-0010	6.870E+0002	3.050E+0002	2.554E-0006	2.665E+0002	9.240E-0001
7.281E-0006	4.010E-0010	6.934E+0002	3.053E+0002	2.578E-0006	2.667E+0002	9.240E-0001
7.259E-0006	3.973E-0010	7.000E+0002	3.057E+0002	2.532E-0006	2.669E+0002	9.240E-0001
7.236E-0006	3.937E-0010	7.065E+0002	3.060E+0002	2.698E-0006	2.671E+0002	9.240E-0001
7.213E-0006	3.899E-0010	7.135E+0002	3.064E+0002	2.653E-0006	2.673E+0002	9.240E-0001
7.191E-0006	3.862E-0010	7.204E+0002	3.068E+0002	2.606E-0006	2.675E+0002	9.240E-0001
7.168E-0006	3.826E-0010	7.273E+0002	3.071E+0002	2.631E-0006	2.677E+0002	9.240E-0001
7.145E-0006	3.790E-0010	7.343E+0002	3.075E+0002	2.730E-0006	2.679E+0002	9.240E-0001
7.122E-0006	3.753E-0010	7.416E+0002	3.078E+0002	2.758E-0006	2.681E+0002	9.240E-0001
7.099E-0006	3.716E-0010	7.491E+0002	3.082E+0002	2.634E-0006	2.683E+0002	9.240E-0001
7.076E-0006	3.681E-0010	7.563E+0002	3.086E+0002	2.736E-0006	2.685E+0002	9.240E-0001
7.053E-0006	3.645E-0010	7.638E+0002	3.089E+0002	2.764E-0006	2.687E+0002	9.240E-0001
7.029E-0006	3.609E-0010	7.715E+0002	3.093E+0002	2.870E-0006	2.689E+0002	9.240E-0001
7.006E-0006	3.572E-0010	7.796E+0002	3.097E+0002	2.742E-0006	2.692E+0002	9.240E-0001
6.983E-0006	3.537E-0010	7.874E+0002	3.101E+0002	2.770E-0006	2.694E+0002	9.240E-0001
6.959E-0006	3.502E-0010	7.953E+0002	3.105E+0002	2.878E-0006	2.696E+0002	9.240E-0001
6.935E-0006	3.466E-0010	8.036E+0002	3.109E+0002	2.908E-0006	2.698E+0002	9.240E-0001
6.912E-0006	3.430E-0010	8.121E+0002	3.113E+0002	2.857E-0006	2.700E+0002	9.240E-0001
6.888E-0006	3.395E-0010	8.205E+0002	3.117E+0002	2.804E-0006	2.702E+0002	9.240E-0001
6.864E-0006	3.361E-0010	8.288E+0002	3.121E+0002	2.916E-0006	2.705E+0002	9.240E-0001
6.840E-0006	3.326E-0010	8.375E+0002	3.125E+0002	3.032E-0006	2.707E+0002	9.240E-0001
6.816E-0006	3.290E-0010	8.467E+0002	3.129E+0002	2.894E-0006	2.709E+0002	9.240E-0001
6.792E-0006	3.256E-0010	8.556E+0002	3.133E+0002	2.924E-0006	2.711E+0002	9.240E-0001
6.768E-0006	3.222E-0010	8.646E+0002	3.137E+0002	3.043E-0006	2.714E+0002	9.240E-0001
6.744E-0006	3.187E-0010	8.741E+0002	3.141E+0002	3.076E-0006	2.716E+0002	9.240E-0001
6.719E-0006	3.152E-0010	8.838E+0002	3.145E+0002	3.021E-0006	2.718E+0002	9.240E-0001
6.695E-0006	3.118E-0010	8.934E+0002	3.149E+0002	2.964E-0006	2.720E+0002	9.240E-0001
6.670E-0006	3.085E-0010	9.029E+0002	3.154E+0002	3.178E-0006	2.723E+0002	9.240E-0001
6.646E-0006	3.050E-0010	9.132E+0002	3.158E+0002	3.122E-0006	2.725E+0002	9.240E-0001
6.621E-0006	3.016E-0010	9.234E+0002	3.162E+0002	3.064E-0006	2.727E+0002	9.240E-0001
6.596E-0006	2.983E-0010	9.336E+0002	3.167E+0002	3.192E-0006	2.730E+0002	9.240E-0001
6.571E-0006	2.949E-0010	9.442E+0002	3.171E+0002	3.133E-0006	2.732E+0002	9.240E-0001
6.546E-0006	2.916E-0010	9.548E+0002	3.175E+0002	3.362E-0006	2.735E+0002	9.240E-0001
6.521E-0006	2.881E-0010	9.663E+0002	3.180E+0002	3.106E-0006	2.737E+0002	9.240E-0001
6.496E-0006	2.849E-0010	9.747E+0002	3.180E+0002	3.231E-0006	2.735E+0002	9.227E-0001
6.471E-0006	2.816E-0010	9.837E+0002	3.180E+0002	3.261E-0006	2.733E+0002	9.214E-0001
6.445E-0006	2.783E-0010	9.928E+0002	3.180E+0002	3.392E-0006	2.731E+0002	9.201E-0001

6.420E-0006	2.749E-0010	1.002E+0003	3.180E+0002	3.222E-0006	2.728E+0002	9.188E-0001
6.394E-0006	2.717E-0010	1.011E+0003	3.180E+0002	3.252E-0006	2.726E+0002	9.175E-0001
6.369E-0006	2.685E-0010	1.020E+0003	3.180E+0002	3.385E-0006	2.724E+0002	9.162E-0001
6.343E-0006	2.652E-0010	1.030E+0003	3.180E+0002	3.417E-0006	2.721E+0002	9.148E-0001
6.317E-0006	2.619E-0010	1.040E+0003	3.180E+0002	3.240E-0006	2.719E+0002	9.134E-0001
6.291E-0006	2.588E-0010	1.050E+0003	3.180E+0002	3.376E-0006	2.717E+0002	9.121E-0001
6.265E-0006	2.556E-0010	1.060E+0003	3.180E+0002	3.408E-0006	2.714E+0002	9.107E-0001
6.239E-0006	2.524E-0010	1.070E+0003	3.180E+0002	3.549E-0006	2.712E+0002	9.092E-0001
6.212E-0006	2.491E-0010	1.081E+0003	3.180E+0002	3.257E-0006	2.709E+0002	9.078E-0001
6.186E-0006	2.461E-0010	1.090E+0003	3.180E+0002	3.507E-0006	2.706E+0002	9.064E-0001
6.159E-0006	2.429E-0010	1.101E+0003	3.180E+0002	3.430E-0006	2.704E+0002	9.049E-0001
6.133E-0006	2.398E-0010	1.112E+0003	3.180E+0002	3.687E-0006	2.701E+0002	9.034E-0001
6.106E-0006	2.365E-0010	1.123E+0003	3.180E+0002	3.385E-0006	2.698E+0002	9.018E-0001
6.079E-0006	2.335E-0010	1.134E+0003	3.180E+0002	3.417E-0006	2.695E+0002	9.004E-0001
6.052E-0006	2.305E-0010	1.144E+0003	3.180E+0002	3.680E-0006	2.692E+0002	8.989E-0001
6.025E-0006	2.273E-0010	1.156E+0003	3.180E+0002	3.582E-0006	2.688E+0002	8.971E-0001
5.998E-0006	2.242E-0010	1.156E+0003	3.180E+0002	3.467E-0006	2.666E+0002	8.900E-0001
5.970E-0006	2.212E-0010	1.156E+0003	3.180E+0002	3.467E-0006	2.644E+0002	8.831E-0001
5.943E-0006	2.182E-0010	1.156E+0003	3.180E+0002	3.582E-0006	2.622E+0002	8.763E-0001
5.915E-0006	2.151E-0010	1.156E+0003	3.180E+0002	3.582E-0006	2.600E+0002	8.692E-0001
5.887E-0006	2.120E-0010	1.156E+0003	3.180E+0002	3.236E-0006	2.577E+0002	8.621E-0001
5.859E-0006	2.092E-0010	1.156E+0003	3.180E+0002	3.467E-0006	2.557E+0002	8.557E-0001
5.831E-0006	2.062E-0010	1.156E+0003	3.180E+0002	3.467E-0006	2.535E+0002	8.489E-0001
5.803E-0006	2.032E-0010	1.156E+0003	3.180E+0002	3.582E-0006	2.514E+0002	8.421E-0001
5.775E-0006	2.001E-0010	1.156E+0003	3.180E+0002	3.236E-0006	2.491E+0002	8.350E-0001
5.746E-0006	1.973E-0010	1.156E+0003	3.180E+0002	3.351E-0006	2.471E+0002	8.286E-0001
5.718E-0006	1.944E-0010	1.156E+0003	3.180E+0002	3.467E-0006	2.450E+0002	8.220E-0001
5.689E-0006	1.914E-0010	1.156E+0003	3.180E+0002	3.467E-0006	2.428E+0002	8.151E-0001
5.660E-0006	1.884E-0010	1.156E+0003	3.180E+0002	3.120E-0006	2.406E+0002	8.083E-0001
5.631E-0006	1.857E-0010	1.156E+0003	3.180E+0002	2.773E-0006	2.387E+0002	8.021E-0001
5.602E-0006	1.833E-0010	1.156E+0003	3.180E+0002	0.000E+0000	2.369E+0002	7.966E-0001

LIST OF REFERENCES

1. Philpott, M., et al., Phase I Report: Integrated Mesoscopic Cooler Circuits (IMCCs), University of Illinois at Urbana-Champaign, 1998.
2. Cohen, R., and E. Groll, "Update on Refrigerant Compressors in Light of CFC Substitutes", Bulletin of the International Institute of Refrigeration, 96-5, pp. 2-19.
3. Purcell, E. M., Electricity and Magnetism, McGraw-Hill, 1985.
4. White, F. M., Viscous Fluid Flow, McGraw-Hill, 1991.
5. White, F. M., Fluid Mechanics, McGraw-Hill, 1994.
6. Gross, W., L. Matsch,V. Castelli, A. Eshel, J. Vohr, and M. Wildmann, Fluid Film Lubrication, Wiley, 1980.
7. Matsuda, R., and S. Fakui, "Asymptotic Analysis of Ultra-Thin Gas Squeeze Film lubrication for Infinitely Large Squeeze Number (Extension of Pan's Theory to the Molecular Gas Film Lubrication Equation)", Journal of Tribology, Vol. 117, January, 1995.
8. Zhang, L., Dan Chao, Shirishi, H., and Trimmer, W., 1992, DSC. Vol. 40, Micromechanical Systems, ASME, pp 149-160.
9. Gupta, R. K., and S. D. Senturia, "Pull-in Time Dynamics as a Measure of Absolute Pressure", Tenth IEEE Intl. Workshop on MEMS, Nagoya, Japan, January 26-30, 1997.